

Heavy-flavor mesons in a hot medium

Glòria Montaña

2023 Dissertation Award in Hadronic Physics

PhD Thesis : Effective-theory description of heavy-flavored hadrons and their properties in a hot medium

arXiv: [2207.10752](https://arxiv.org/abs/2207.10752)



UNIVERSITAT DE
BARCELONA



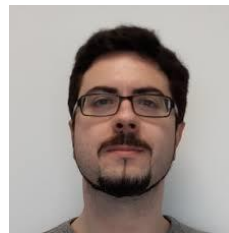
EXCELENCIA
MARIA
DE MAEZTU



Dra Àngels Ramos



Dra Laura Tolós



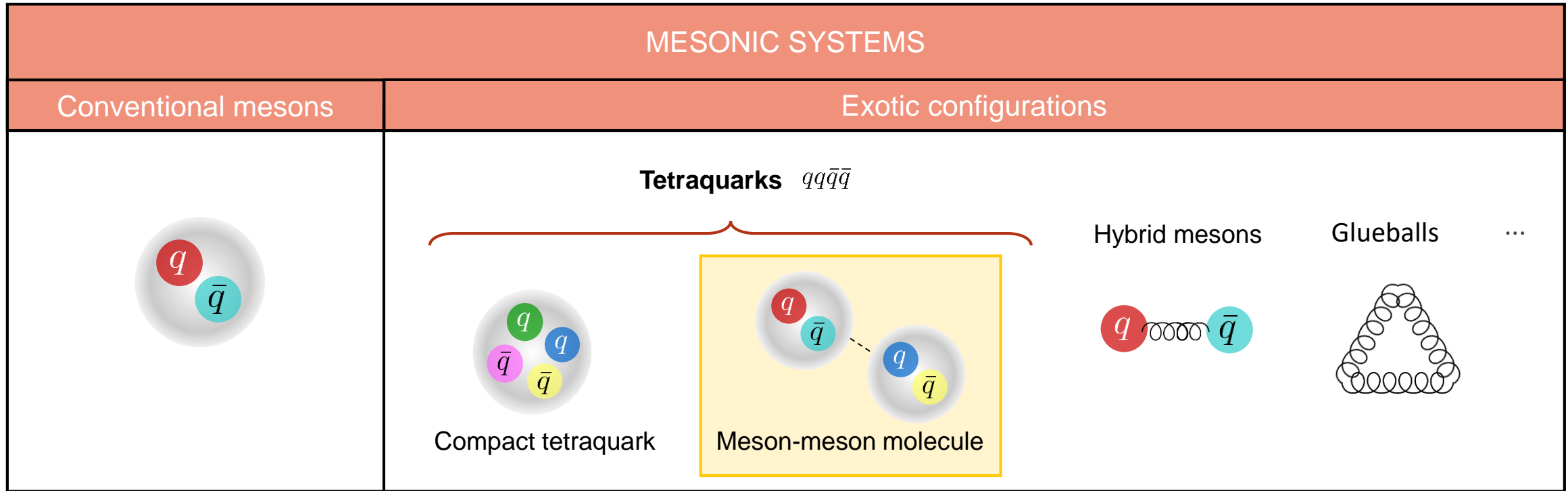
Dr Juan M. Torres-Rincon



OUTLINE

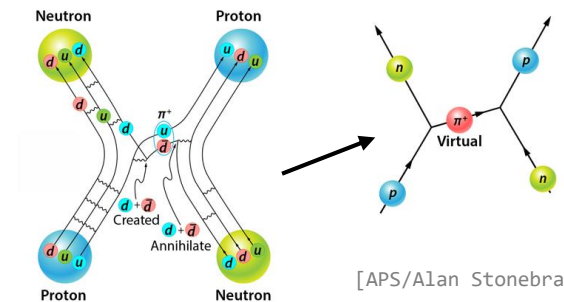
1. Introduction & Motivation: Why heavy mesons? Why hot medium?
2. Thermal EFT for heavy mesons
3. Open heavy-flavor mesons: Thermal properties
4. Transport coefficients
5. X(3872) & X(4014)
6. Summary

Introduction: Exotic hadrons and hadronic molecules



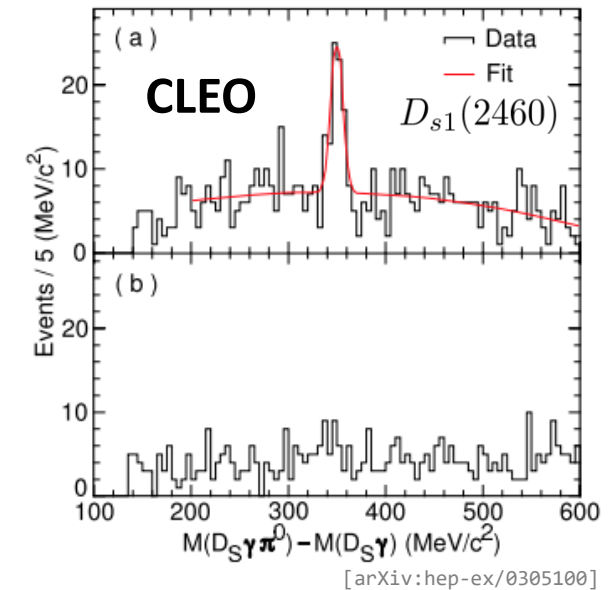
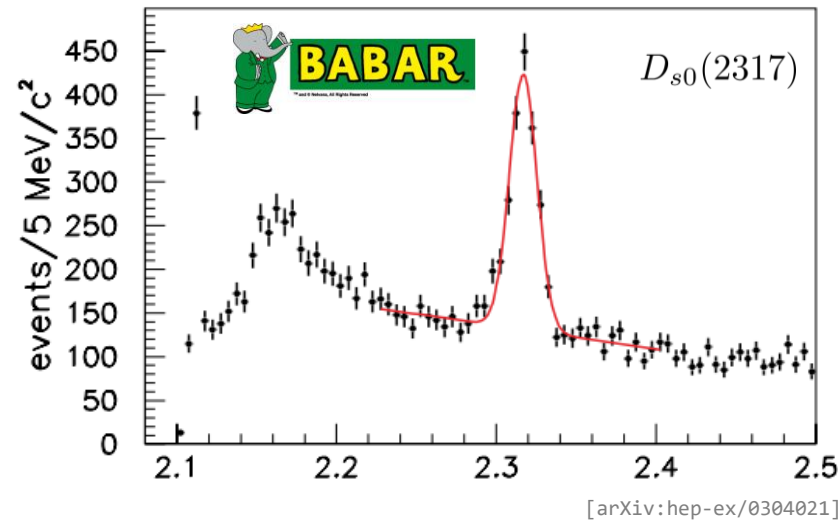
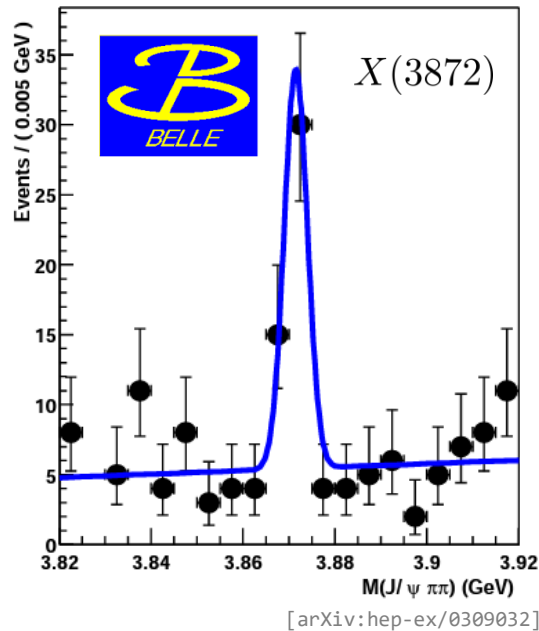
Hadronic molecules are deuteron-like quasi-bound states of two hadrons

- Dynamically generated via multiple scattering of their hadronic components
- Located near threshold
- Studied using **effective hadronic theories**: hadronic degrees of freedom



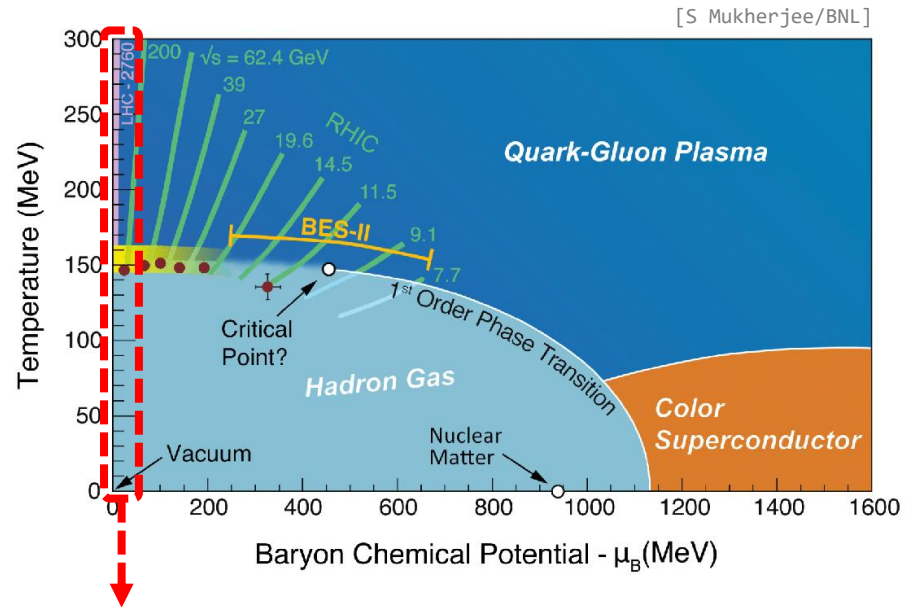
Why heavy mesons?

- 2003 : discovery of the first **heavy exotica** candidates (with at least one heavy quark, c or b)



- Confirmed and extensively studied in electron-positron and proton-(anti)proton colliders (Belle, Babar, BESIII, CLEO, CDF, CO, LHCb...)
- Their internal structure is still unknown (compact tetraquark, molecule, admixture?)
- 2021 : first evidence for $X(3872)$ production in Pb-Pb collisions by the CMS collaboration [Phys. Rev. Lett., 128 (2022) 032001]
- Future femtoscopy measurements └──────────┬──────────┘ New opportunities to probe the nature of exotic states

Why hot medium?



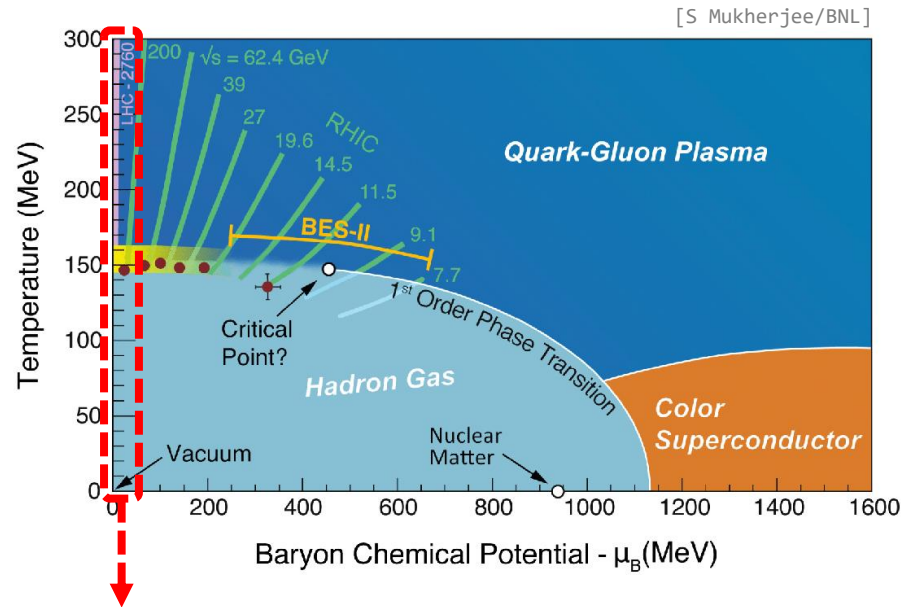
Theoretical tools to study QCD matter at high temperatures:

- Perturbative theories (very high T)
- Lattice QCD
- **Non-perturbative effective hadronic theories** (below transition temperature T_c)

High-energy HICs

- LHC@CERN
- RHIC@BNL
- Heavy quarks are created in the initial stage of the collision
- Due to the large mass and relaxation time, heavy-flavor mesons are a powerful probe of the QGP
- The properties of heavy mesons (masses and decay widths) are modified in hot matter

Why hot medium?



Theoretical tools to study QCD matter at high temperatures:

- Perturbative theories (very high T)
- Lattice QCD
- **Non-perturbative effective hadronic theories** (below transition temperature T_c)

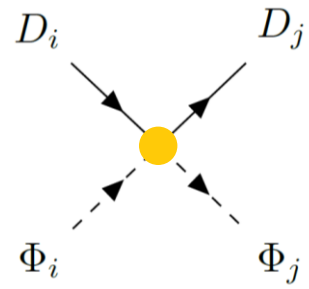
High-energy HICs

- LHC@CERN
- RHIC@BNL
- Heavy quarks are created in the initial stage of the collision
- Due to the large mass and relaxation time, heavy-flavor mesons are a powerful probe of the QGP
- The properties of heavy mesons (masses and decay widths) are modified in hot matter

Our approach :

- Mesonic matter at temperature $0 < T < T_c$ and vanishing baryon density \rightarrow mostly pions (thermal equilibrium)
- Heavy mesons behave as Brownian particles scattering off the light mesons
- New processes are available: production and absorption of thermal mesons

Thermal effective field theory for heavy mesons

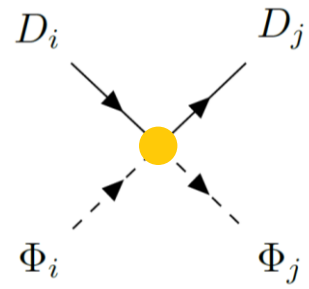


Interaction between open heavy-flavor mesons and Goldstone bosons given by **heavy-meson effective theory (HMET)** (in vacuum)

[Wise (1992), Burdman and Donoghue (1992), Casalbuoni, Deandrea, Di Bartolomeo et al (1997), Liu, Orginos, Guo, Hanhart and Meißner (2013), Tolos and Torres-Rincon (2013), Albaladejo, Fernandez-Soler, Guo and Nieves (2017), Guo, Liu, Meißner, Oller and Ruscetsky (2019)]

- Chiral symmetry in the limit $m_u, m_d, m_s \rightarrow 0$
- Heavy-quark symmetries in the limit $m_c, m_b \rightarrow \infty$
 - Heavy-quark spin-flavor symmetry (HQSF): $\{c \uparrow, c \downarrow, b \uparrow, b \downarrow\} \quad \{D, D^*, \bar{B}, \bar{B}^*\}$

Thermal effective field theory for heavy mesons



Interaction between open heavy-flavor mesons and Goldstone bosons given by **heavy-meson effective theory (HMET)** (in vacuum)

[Wise (1992), Burdman and Donoghue (1992), Casalbuoni, Deandrea, Di Bartolomeo et al (1997), Liu, Orginos, Guo, Hanhart and Meißner (2013), Tolos and Torres-Rincon (2013), Albaladejo, Fernandez-Soler, Guo and Nieves (2017), Guo, Liu, Meißner, Oller and Rusetsky (2019)]

- Chiral symmetry in the limit $m_u, m_d, m_s \rightarrow 0$
- Heavy-quark symmetries in the limit $m_c, m_b \rightarrow \infty$
 - Heavy-quark spin-flavor symmetry (HQSF): $\{c \uparrow, c \downarrow, b \uparrow, b \downarrow\} \quad \{D, D^*, \bar{B}, \bar{B}^*\}$

Lagrangian at NLO in the chiral expansion and LO in the heavy-quark mass expansion:

Tree-level scattering amplitude:

$$V^{ij}(s, t, u) = \frac{1}{f_\pi^2} \left[\frac{C_{\text{LO}}^{ij}}{4} (s - u) - 4C_0^{ij} h_0 + 2C_1^{ij} h_1 - 2C_{24}^{ij} \left(2h_2 (p_2 \cdot p_4) + h_4 \left((p_1 \cdot p_2)(p_3 \cdot p_4) + (p_1 \cdot p_4)(p_2 \cdot p_3) \right) \right) + 2C_{35}^{ij} \left(h_3 (p_2 \cdot p_4) + h_5 \left((p_1 \cdot p_2)(p_3 \cdot p_4) + (p_1 \cdot p_4)(p_2 \cdot p_3) \right) \right) \right]$$

C_k^{ij} isospin coefficients

LECs fitted to lattice QCD data

[Guo, Liu, Meißner, Oller and Rusetsky (2019)]

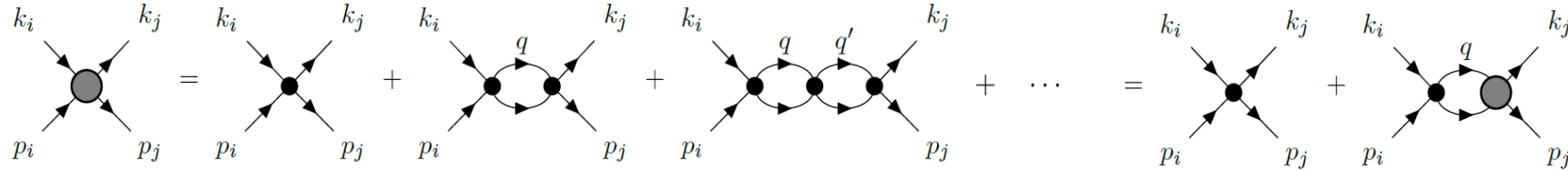
At LO in HQSFS: $h_{0,\dots,3}^B \hat{M}_B^{-1} = h_{0,\dots,3}^D \hat{M}_D^{-1}$, $h_{4,5}^B \hat{M}_B = h_{4,5}^D \hat{M}_D$

Recent results for $D\pi$ and DK from femtoscopy from ALICE pp , $\sqrt{s} = 13$ TeV at high multiplicity

[ALI-PREL-513658]

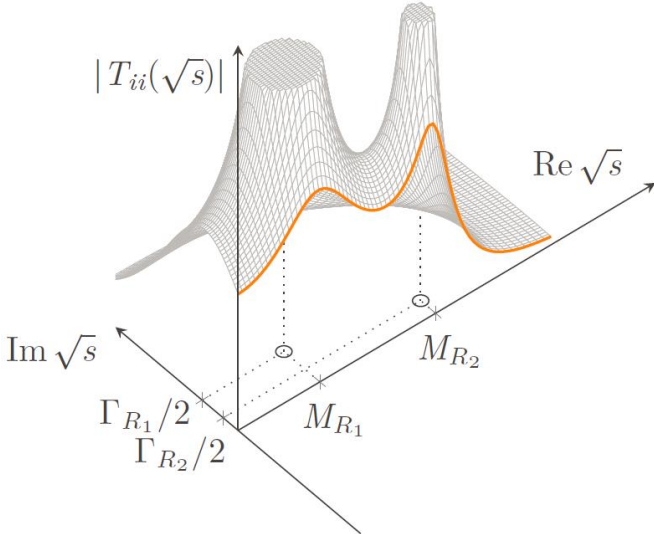
Thermal effective field theory for heavy mesons

Unitarization: on-shell Bethe-Salpeter equation in coupled channels



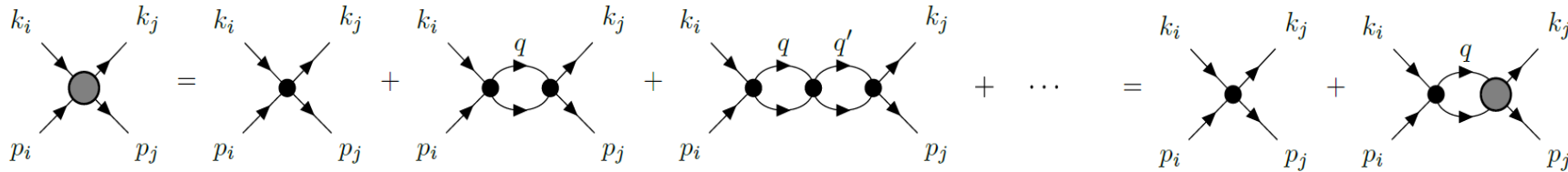
$$T = \frac{V}{1 - VG} \quad \longrightarrow \quad \text{Two-meson propagator or loop function} \quad G_k(s) = i \int \frac{d^4q}{(2\pi)^4} \frac{1}{q^2 - m_D^2 + i\epsilon} \frac{1}{(p - q)^2 - m_\Phi^2 + i\epsilon}$$

regularized with a momentum cut-off



Thermal effective field theory for heavy mesons

Unitarization: on-shell Bethe-Salpeter equation in coupled channels

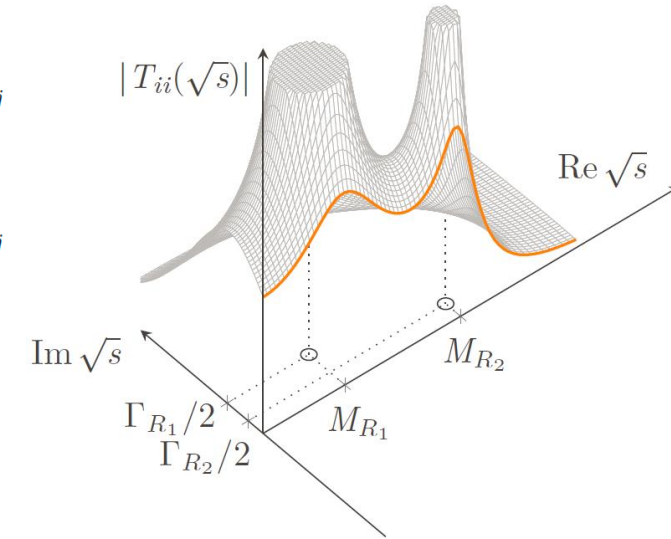


$$T = \frac{V}{1 - VG}$$

Two-meson propagator or loop function

$$G_k(s) = i \int \frac{d^4 q}{(2\pi)^4} \frac{1}{q^2 - m_D^2 + i\varepsilon} \frac{1}{(p - q)^2 - m_\Phi^2 + i\varepsilon}$$

regularized with a momentum cut-off



Imaginary time formalism

- Sum over Matsubara frequencies $q^0 \rightarrow i\omega_n = i \frac{2n\pi}{\beta}$ (bosons), $\int \frac{d^4 q}{(2\pi)^4} \rightarrow \frac{1}{\beta} \sum_n \int \frac{d^3 q}{(2\pi)^3}$
- Thermal production and absorption processes weighted by Bose-Einstein distribution functions $f(\omega, T) = \frac{1}{e^{\omega/T} - 1}$

Dressing of the mesons in the loop functions with their spectral functions

- Self-energy corrections to the heavy meson propagator
- Pion mass slightly varies below $T_c \rightarrow$ Approximation: only the heavy meson is dressed

Thermal effective field theory for heavy mesons

Loop function

$$G_{D\Phi}(E, \vec{p}; T) = \int \frac{d^3q}{(2\pi)^3} \int d\omega \int d\omega' \frac{S_D(\omega, \vec{q}; T) S_\Phi(\omega', \vec{p} - \vec{q}; T)}{E - \omega - \omega' + i\epsilon} [1 + f(\omega, T) + f(\omega', T)]$$

Thermal effective field theory for heavy mesons

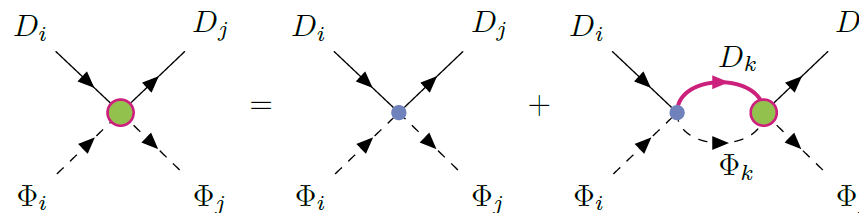
Loop function



Unitarized amplitude

$$G_{D\Phi}(E, \vec{p}; T) = \int \frac{d^3q}{(2\pi)^3} \int d\omega \int d\omega' \frac{S_D(\omega, \vec{q}; T) S_\Phi(\omega', \vec{p} - \vec{q}; T)}{E - \omega - \omega' + i\epsilon} [1 + f(\omega, T) + f(\omega', T)]$$

$$T_{ij} = V_{ij} + V_{ik} G_k T_{kj}$$



Thermal effective field theory for heavy mesons

Loop function



Unitarized amplitude

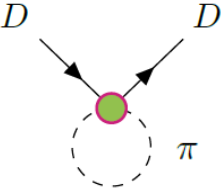


Self-energy

$$G_{D\Phi}(E, \vec{p}; T) = \int \frac{d^3q}{(2\pi)^3} \int d\omega \int d\omega' \frac{S_D(\omega, \vec{q}; T) S_\Phi(\omega', \vec{p} - \vec{q}; T)}{E - \omega - \omega' + i\epsilon} [1 + f(\omega, T) + f(\omega', T)]$$

$$T_{ij} = V_{ij} + V_{ik} G_k T_{kj}$$

$$\Pi_D(\omega, \vec{q}; T) = \frac{1}{\pi} \int \frac{d^3q'}{(2\pi)^3} \int dE \frac{\omega - \omega_\Phi}{\omega_\Phi} \frac{f(E, T) - f(\omega_\Phi, T)}{\omega^2 - (\omega_\Phi - E)^2 + \text{sgn}(\omega) i\epsilon} \text{Im } T_{D\Phi}(E, \vec{p}; T)$$



Thermal effective field theory for heavy mesons

Loop function

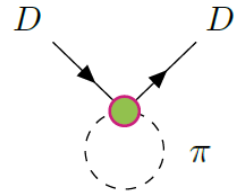
$$G_{D\Phi}(E, \vec{p}; T) = \int \frac{d^3q}{(2\pi)^3} \int d\omega \int d\omega' \frac{S_D(\omega, \vec{q}; T) S_\Phi(\omega', \vec{p} - \vec{q}; T)}{E - \omega - \omega' + i\epsilon} [1 + f(\omega, T) + f(\omega', T)]$$

Unitarized amplitude

$$T_{ij} = V_{ij} + V_{ik} G_k T_{kj}$$

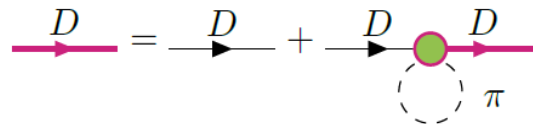
Self-energy

$$\Pi_D(\omega, \vec{q}; T) = \frac{1}{\pi} \int \frac{d^3q'}{(2\pi)^3} \int dE \frac{\omega - \omega_\Phi}{\omega_\Phi} \frac{f(E, T) - f(\omega_\Phi, T)}{\omega^2 - (\omega_\Phi - E)^2 + \text{sgn}(\omega) i\epsilon} \text{Im } T_{D\Phi}(E, \vec{p}; T)$$

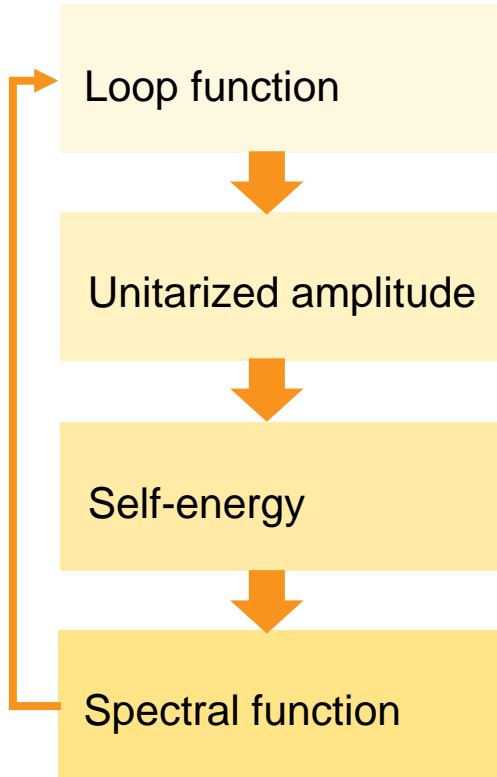


Spectral function

$$S_D(\omega, \vec{q}; T) = -\frac{1}{\pi} \text{Im } \mathcal{D}_D(\omega, \vec{q}; T) = -\frac{1}{\pi} \text{Im} \left(\frac{1}{\omega^2 - \vec{q}^2 - m_D^2 - \Pi_D(\omega, \vec{q}; T)} \right)$$



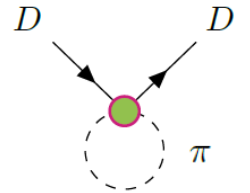
Thermal effective field theory for heavy mesons



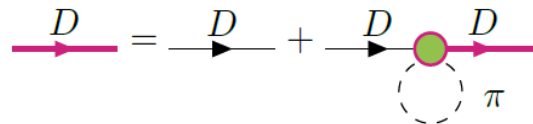
$$G_{D\Phi}(E, \vec{p}; T) = \int \frac{d^3q}{(2\pi)^3} \int d\omega \int d\omega' \frac{S_D(\omega, \vec{q}; T) S_\Phi(\omega', \vec{p} - \vec{q}; T)}{E - \omega - \omega' + i\epsilon} [1 + f(\omega, T) + f(\omega', T)]$$

$$T_{ij} = V_{ij} + V_{ik} G_k T_{kj}$$

$$\Pi_D(\omega, \vec{q}; T) = \frac{1}{\pi} \int \frac{d^3q'}{(2\pi)^3} \int dE \frac{\omega - \omega_\Phi}{\omega_\Phi} \frac{f(E, T) - f(\omega_\Phi, T)}{\omega^2 - (\omega_\Phi - E)^2 + \text{sgn}(\omega) i\epsilon} \text{Im } T_{D\Phi}(E, \vec{p}; T)$$



$$S_D(\omega, \vec{q}; T) = -\frac{1}{\pi} \text{Im } \mathcal{D}_D(\omega, \vec{q}; T) = -\frac{1}{\pi} \text{Im} \left(\frac{1}{\omega^2 - \vec{q}^2 - m_D^2 - \Pi_D(\omega, \vec{q}; T)} \right)$$

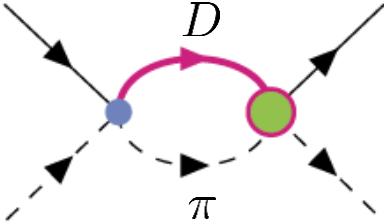
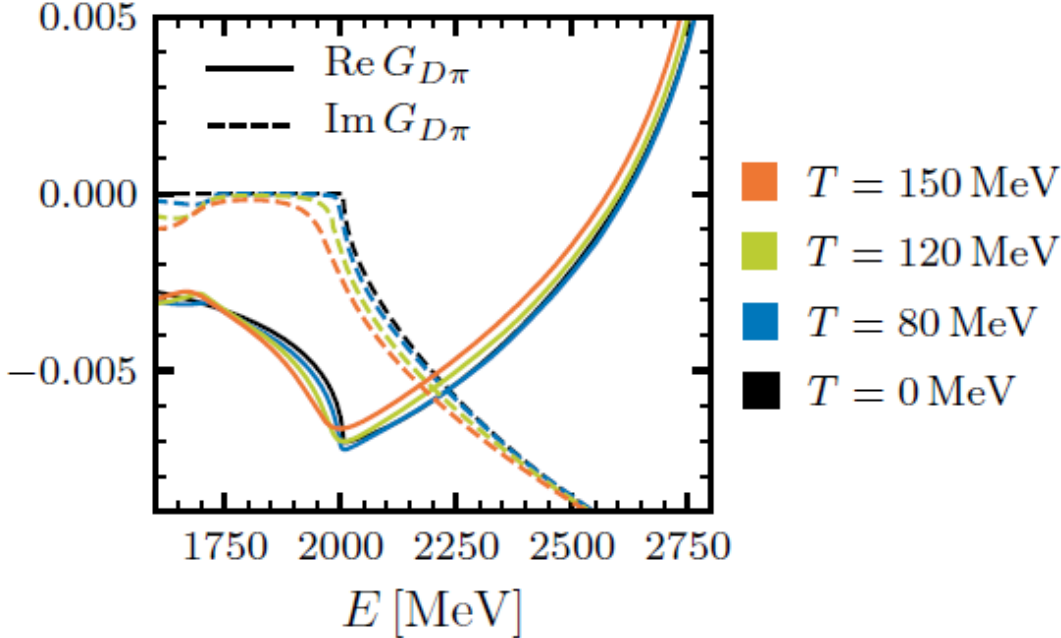
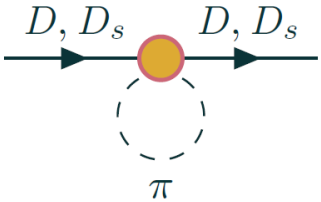


Set of coupled equations \longrightarrow solved self-consistently

Thermal loop function

[GM, A. Ramos, L. Tolos, J.M. Torres-Rincon, *Phys. Lett. B* 806 (2020) 135464, *Phys. Rev. D* 102 (2020) 9, 096020]

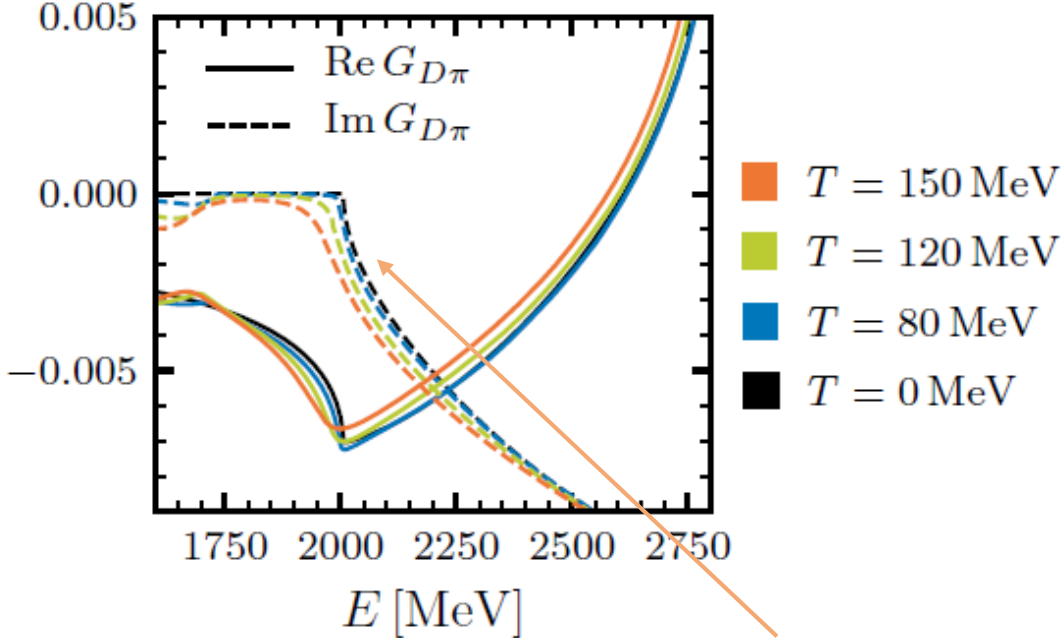
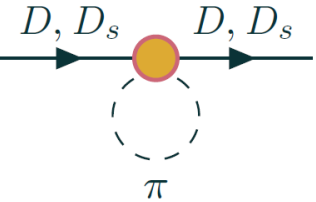
Pionic bath



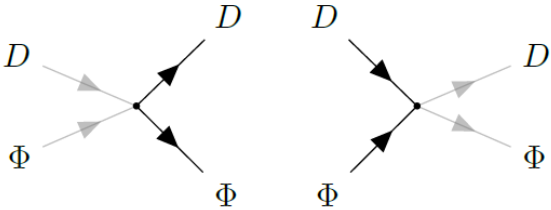
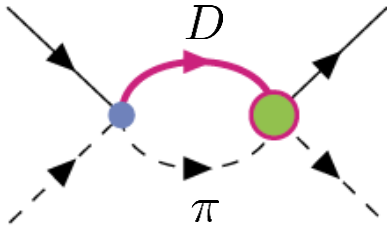
Thermal loop function

[GM, A. Ramos, L. Tolos, J.M. Torres-Rincon, *Phys. Lett. B* 806 (2020) 135464, *Phys. Rev. D* 102 (2020) 9, 096020]

Pionic bath



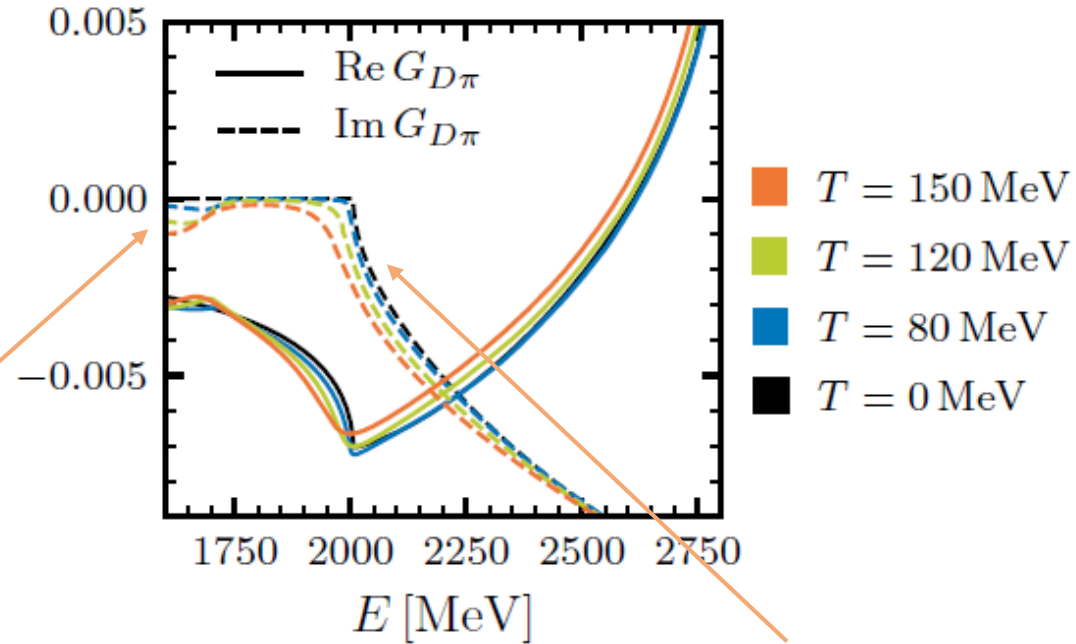
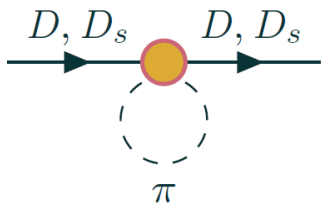
Unitary cut
 $|E| \geq (m_D + m_\pi)$



Thermal loop function

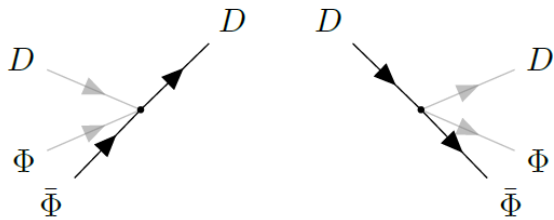
[GM, A. Ramos, L. Tolos, J.M. Torres-Rincon, *Phys. Lett. B* 806 (2020) 135464, *Phys. Rev. D* 102 (2020) 9, 096020]

Pionic bath



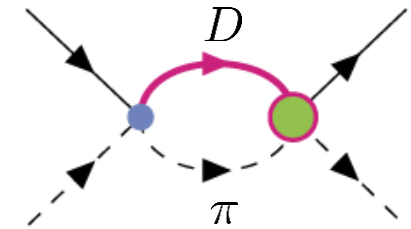
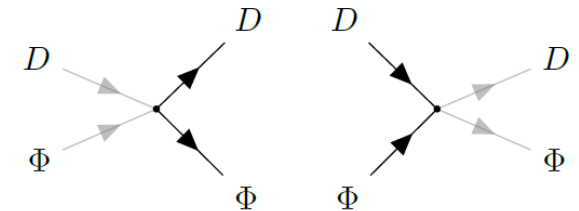
Landau cut

$$|E| \leq (m_D - m_\pi)$$



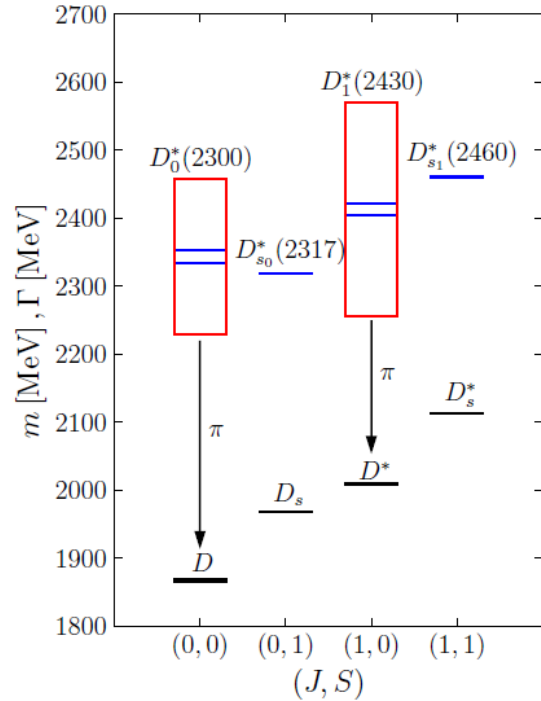
Unitary cut

$$|E| \geq (m_D + m_\pi)$$



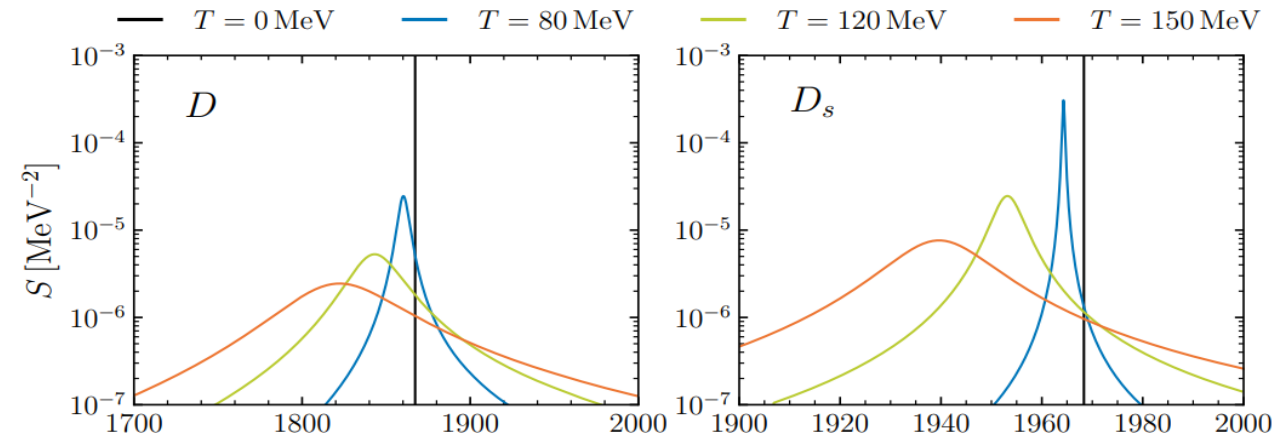
Open heavy-flavor mesons

[GM, A. Ramos, L. Tolos, J.M. Torres-Rincon, *Phys. Lett. B* 806 (2020) 135464, *Phys. Rev. D* 102 (2020) 9, 096020]



Ground-state spectral functions:

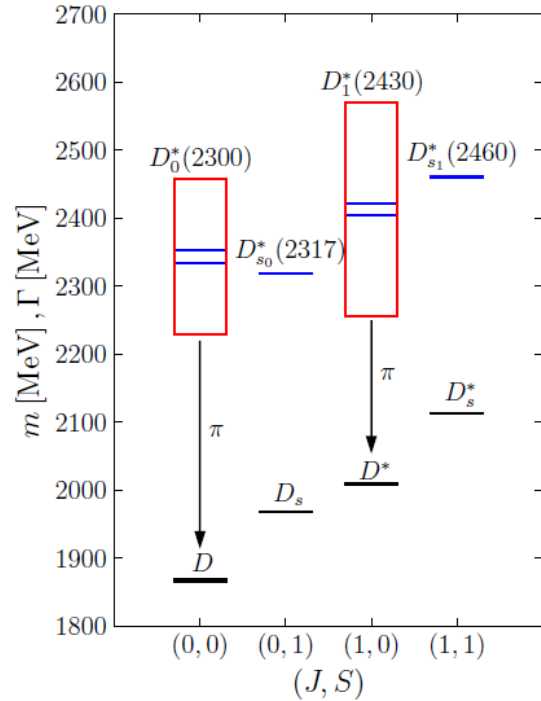
$$S_D(\omega, \vec{q}; T) = -\frac{1}{\pi} \text{Im} \left(\frac{1}{\omega^2 - \vec{q}^2 - m_D^2 - \Pi_D(\omega, \vec{q}; T)} \right)$$



$J^P = 0^-$

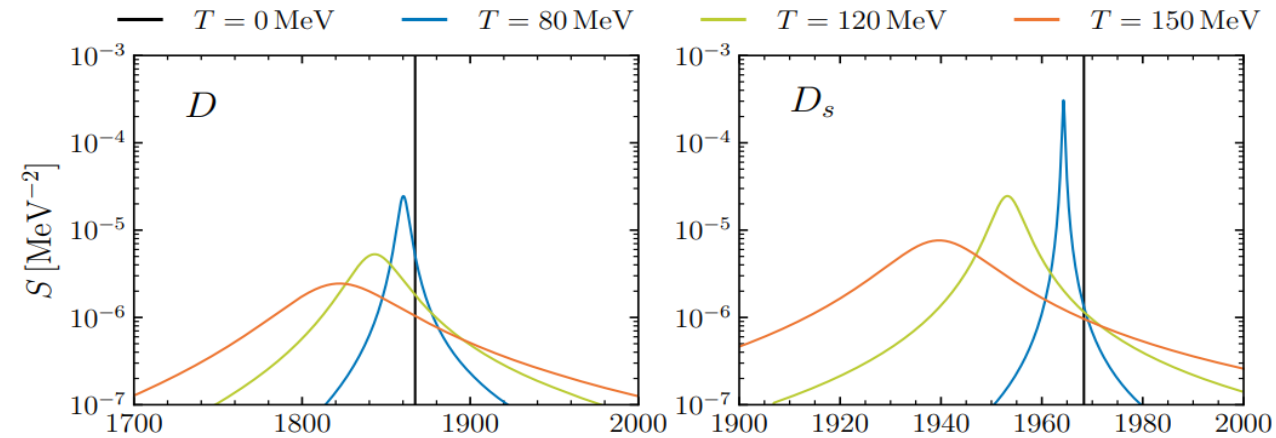
Open heavy-flavor mesons

[GM, A. Ramos, L. Tolos, J.M. Torres-Rincon, *Phys. Lett. B* 806 (2020) 135464, *Phys. Rev. D* 102 (2020) 9, 096020]



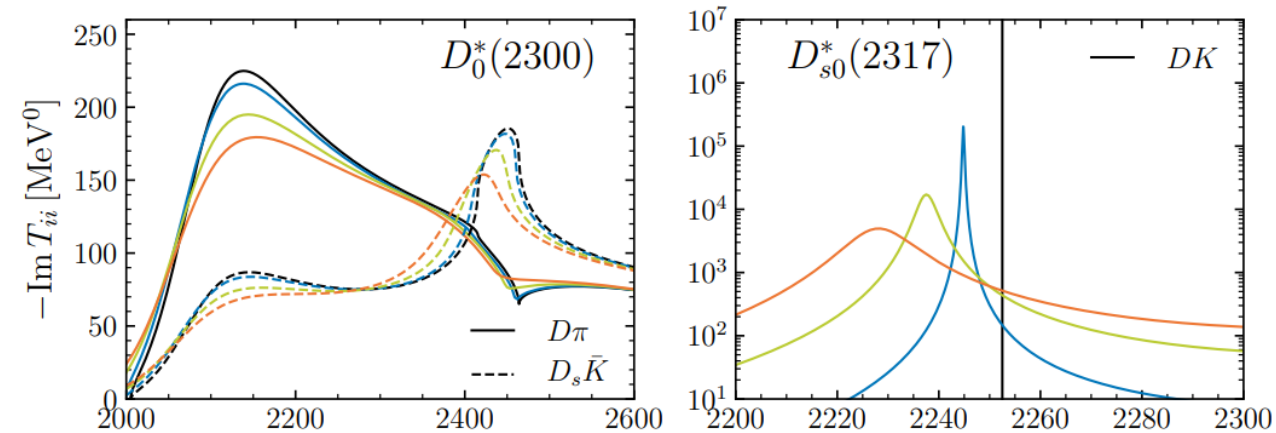
Ground-state spectral functions:

$$S_D(\omega, \vec{q}; T) = -\frac{1}{\pi} \text{Im} \left(\frac{1}{\omega^2 - \vec{q}^2 - m_D^2 - \Pi_D(\omega, \vec{q}; T)} \right)$$



$J^P = 0^-$

Dynamically generated states:



$J^P = 0^+$

We have also investigated the thermal modification of the 1^\pm and bottom counterparts

In vacuum ($T = 0$)

$D_0^*(2300)$: Two-pole structure

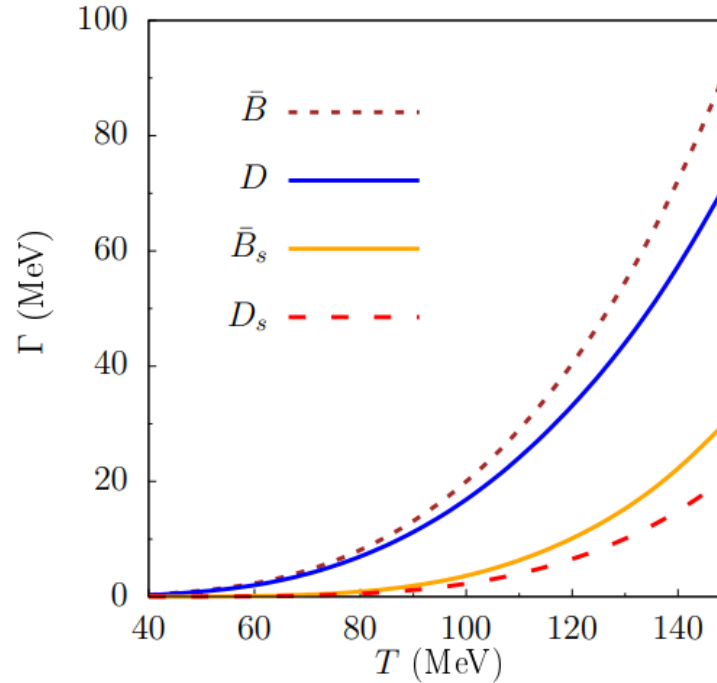
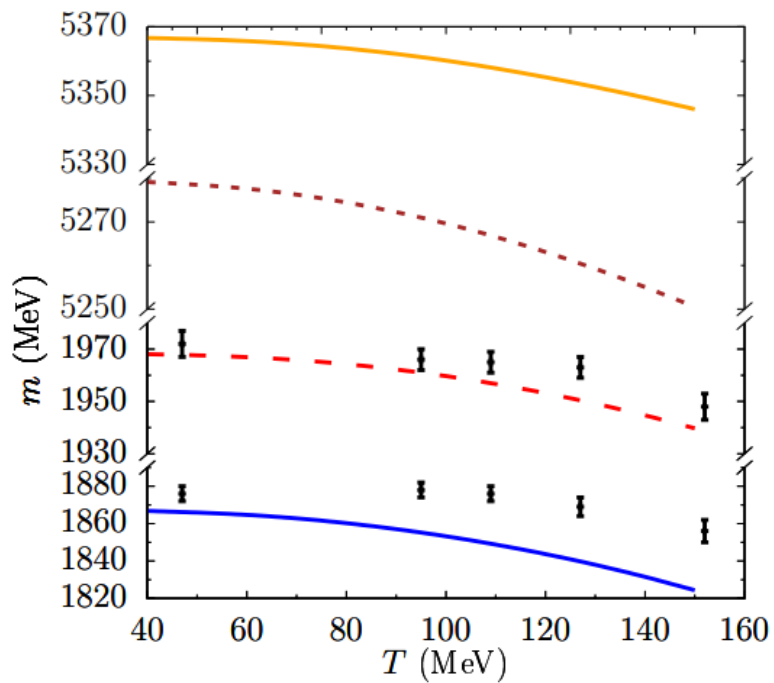
[Albaladejo et al., *Phys.Lett.B* 767 (2017) 465]

$D_{s0}^*(2317)$: Bound state

Thermal masses and widths

[GM, A. Ramos, L. Tolos, J.M. Torres-Rincon, *Phys. Lett. B* 806 (2020) 135464, *Phys. Rev. D* 102 (2020) 9, 096020]

The thermal properties can be directly obtained from the spectral functions



Our results:

- reduction of the in-medium mass
 - thermal widening
- with increasing temperature

Also, reduction of the mass of the D and D_s with increasing temperature from lattice-QCD data

[G. Aarts et al., 2209.14681]

Transport coefficients of off-shell heavy mesons

Fokker-Planck equation (from Kadanoff-Baym approach)

$$\frac{\partial}{\partial t} G_D^<(t, k) = \frac{\partial}{\partial k^i} \left\{ \hat{A}(k; T) k^i G_D^<(t, k) + \frac{\partial}{\partial k^j} \left[\hat{B}_0(k; T) \Delta^{ij} + \hat{B}_1(k; T) \frac{k^i k^j}{\vec{k}^2} \right] G_D^<(t, k) \right\} \quad \text{with } \Delta^{ij} = \delta^{ij} - k^i k^j / \vec{k}^2$$

Green's function $iG_D^<(t, k) = 2\pi S_D(t, k^0, \vec{k}) f_D(t, k^0)$

Off-shell transport coefficients

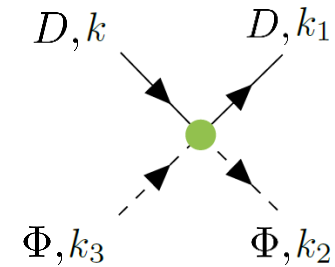
- Drag force coefficient:

$$\hat{A}(k^0, \vec{k}; T) \equiv \left\langle 1 - \frac{\vec{k} \cdot \vec{k}_1}{\vec{k}^2} \right\rangle$$

- Momentum diffusion coefficients:

$$\hat{B}_0(k^0, \vec{k}; T) \equiv \frac{1}{4} \left\langle \vec{k}_1^2 - \frac{(\vec{k} \cdot \vec{k}_1)^2}{\vec{k}^2} \right\rangle$$

$$\hat{B}_1(k^0, \vec{k}; T) \equiv \frac{1}{2} \left\langle \frac{[\vec{k} \cdot (\vec{k} - \vec{k}_1)]^2}{\vec{k}^2} \right\rangle$$



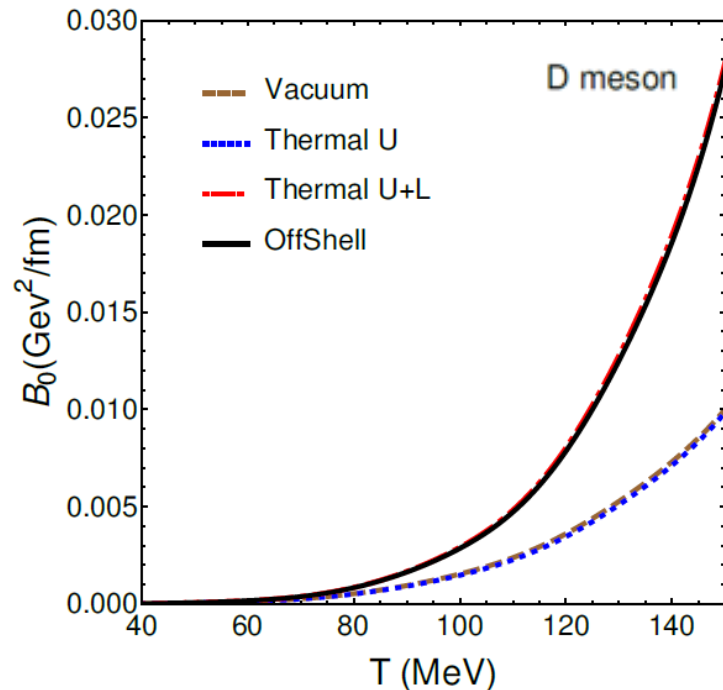
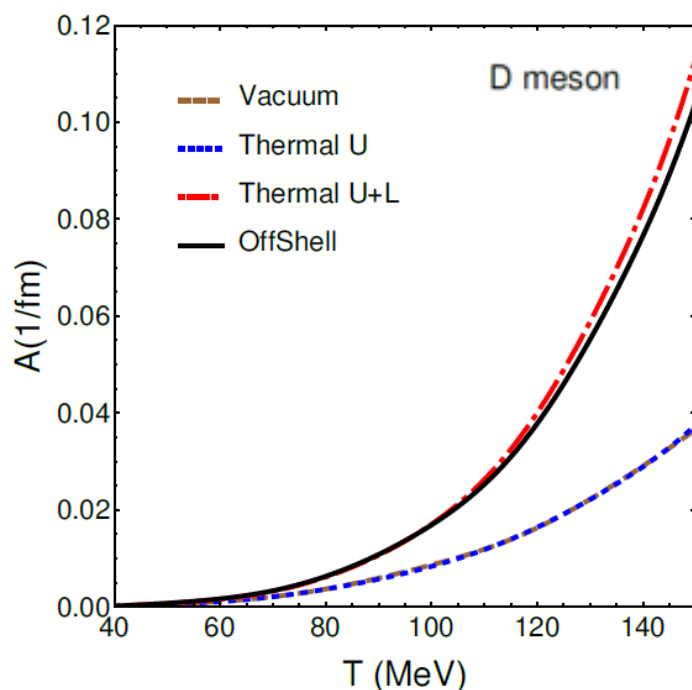
- Thermal effects in $|T|^2$ and E_k
- Landau cut contribution
- Off-shell effects

with

$$\begin{aligned} \langle \mathcal{F}(\vec{k}, \vec{k}_1) \rangle &= \frac{1}{2k^0} \sum_{\lambda, \lambda' = \pm} \lambda \lambda' \int_{-\infty}^{\infty} dk_1^0 \int \prod_{i=1}^3 \frac{d^3 k_i}{(2\pi)^3} \frac{1}{2E_2 2E_3} S_D(k_1^0, \vec{k}_1) (2\pi)^4 \delta^{(3)}(\vec{k} + \vec{k}_3 - \vec{k}_1 - \vec{k}_2) \\ &\times \delta(k^0 + \lambda' E_3 - \lambda E_2 - k_1^0) \left| T(k^0 + \lambda' E_3, \vec{k} + \vec{k}_3) \right|^2 f^{(0)}(\lambda' E_3) \tilde{f}^{(0)}(\lambda E_2) \tilde{f}^{(0)}(k_1^0) \mathcal{F}(\vec{k}, \vec{k}_1) \end{aligned}$$

Drag force and momentum diffusion coefficients

[J.M. Torres-Rincon, GM, A. Ramos, L. Tolos, Phys.Rev.C 105 (2022)]



Drag force A

Momentum diffusion
(longitudinal B_0 and transverse B_1)

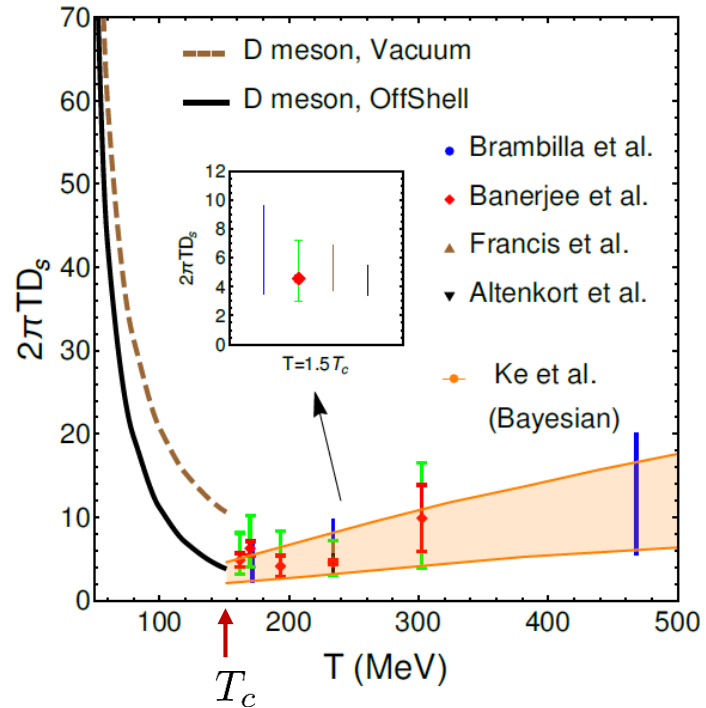
In the static limit $\vec{k} \rightarrow 0$, $B_0 = B_1$

- Increase with temperature
- **Vacuum** vs **Thermal U**: Thermal effects in the amplitudes are small
- **Thermal U** vs **Thermal U+L**: The Landau contribution is very important at finite temperature
- **Thermal U+L** vs **OffShell**: Off-shell effects are small
- The main contribution comes from the pions in the bath

Spatial diffusion coefficient

$$2\pi T D_s(T) = \lim_{\vec{k} \rightarrow 0} \frac{2\pi T^3}{B_0(\vec{k}; T)}$$

[J.M. Torres-Rincon, GM, A. Ramos, L. Tolos, Phys.Rev.C 105 (2022)]



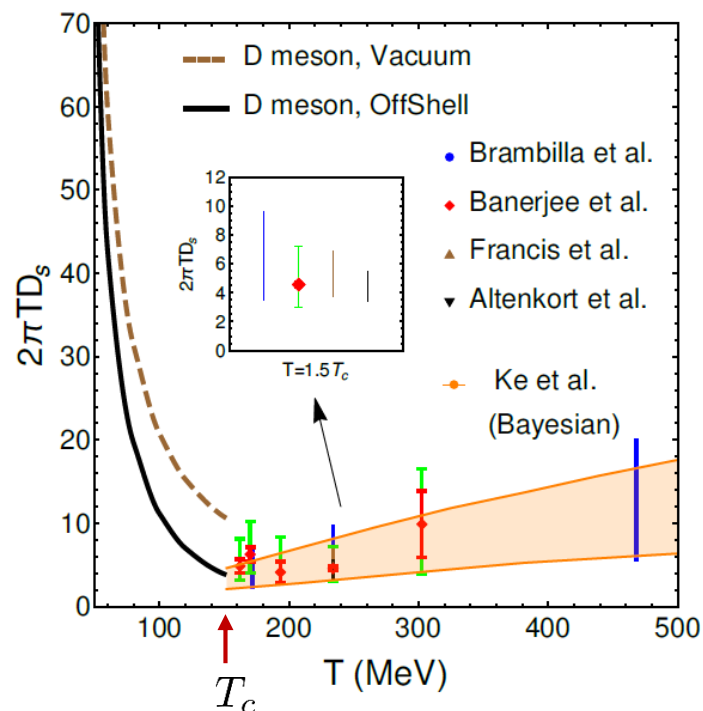
Comparison with:

- Lattice QCD calculations [N. Brambilla et al. Phys. Rev. D102, 074503 (2020)]
[I.D. Banerjee et al. Phys. Rev. D85, 014510 (2012)]
[I.A. Francis et al. Phys. Rev. D92, 116003 (2015)]
[I.L. Altenkort et al. Phys. Rev. D103, 014511 (2021)]
- Bayesian analysis of HICs [W. Ke et al. Phys. Rev. C98, 064901 (2018)]

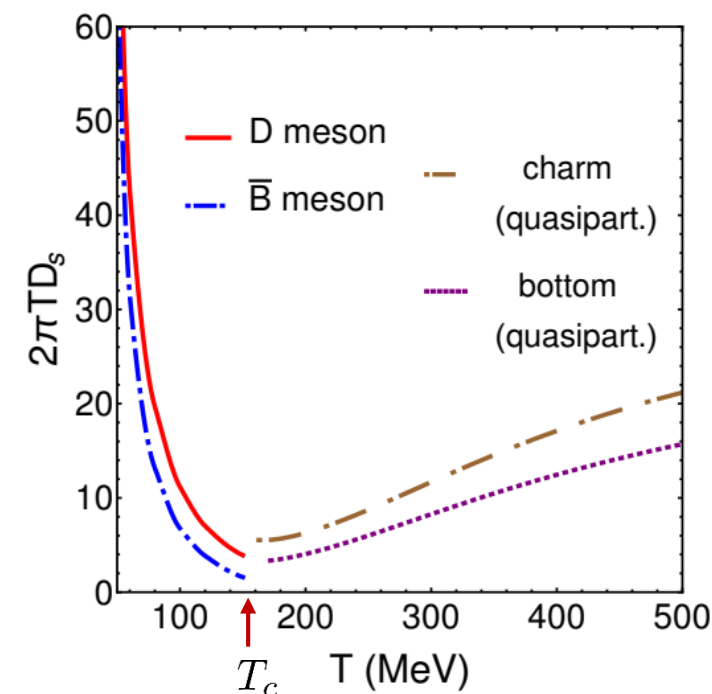
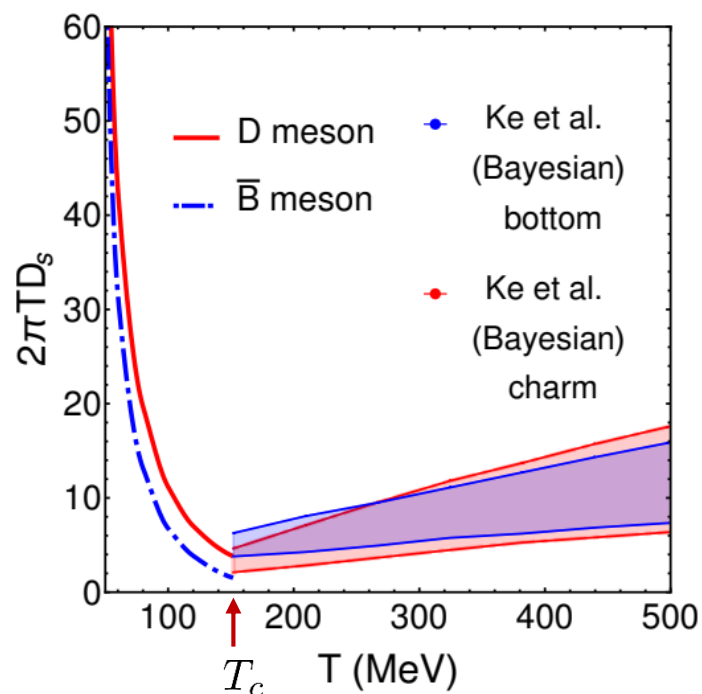
Spatial diffusion coefficient

$$2\pi T D_s(T) = \lim_{\vec{k} \rightarrow 0} \frac{2\pi T^3}{B_0(\vec{k}; T)}$$

[J.M. Torres-Rincon, GM, A. Ramos, L. Tolos, Phys.Rev.C 105 (2022)]



Charm vs Bottom



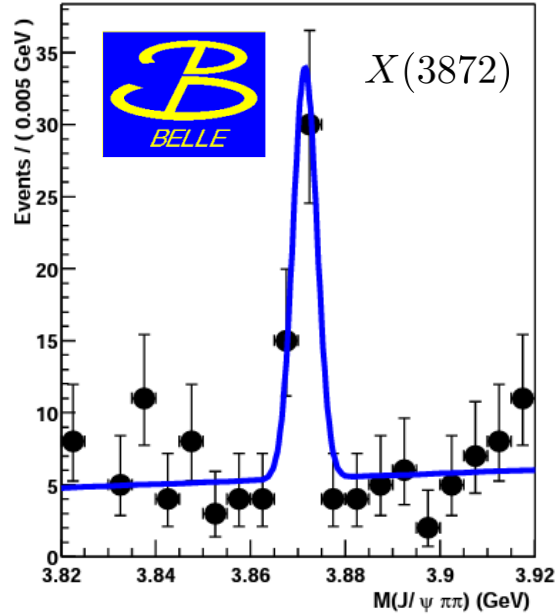
Comparison with:

- Lattice QCD calculations [N. Brambilla et al. Phys. Rev. D102, 074503 (2020)]
[I.D. Banerjee et al. Phys. Rev. D85, 014510 (2012)]
[I.A. Francis et al. Phys. Rev. D92, 116003 (2015)]
[I.L. Altenkort et al. Phys. Rev. D103, 014511 (2021)]
- Bayesian analysis of HICs [W. Ke et al. Phys. Rev. C98, 064901 (2018)]

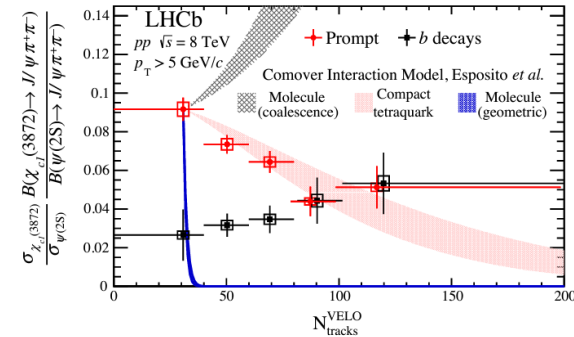
Comparison with:

- Quasiparticle model [Phys. Rev. D94.11 (2016), 114039.]

X(3872) and X(4014)

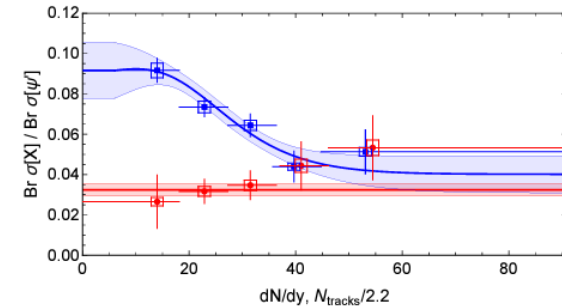


- 2003: $X(3872)$, a.k.a. $\chi_{c1}(3872)$, discovered by Belle [PRL 91 (2003) 262001]
- 2013: quantum numbers determined by LHCb: $J^{PC} = 1^{++}$ [PRL 110 (2013) 222001]
- Its internal structure remains under debate
- Its prompt production in HICs provides an alternative probe to its internal structure



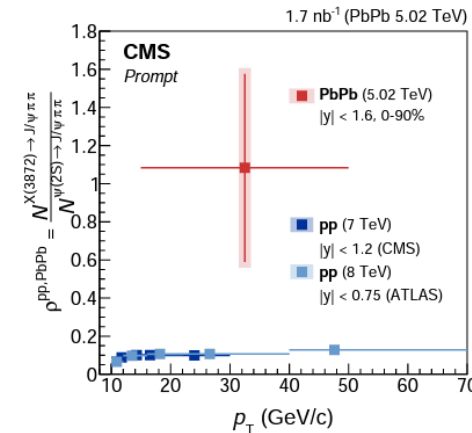
[PRL 126 (2021) 9, 092001]

[Esposito *et al.* (2021)]

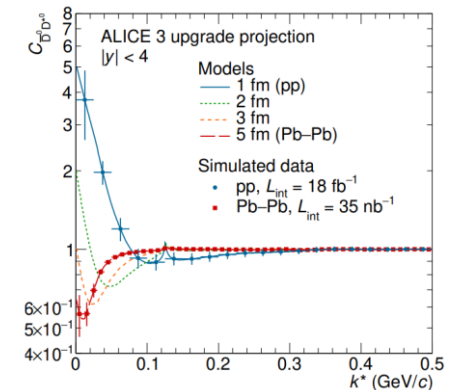


A different model for calculating breakup cross section

[Braaten *et al.* (2021)]

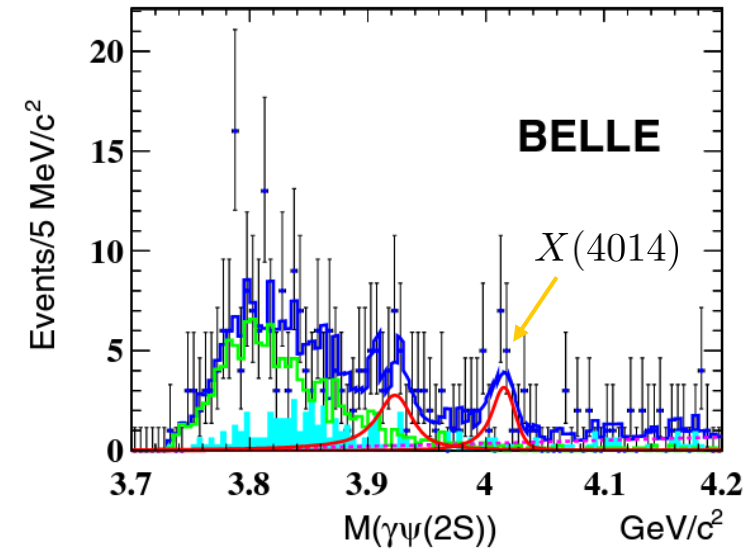
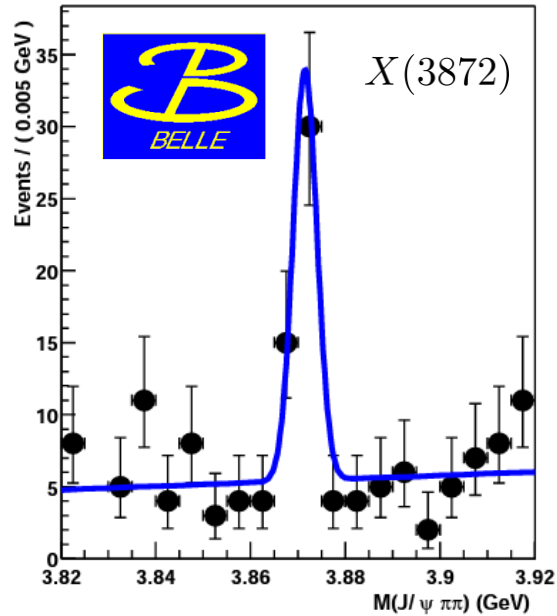


[PRL 128 (2022) 3, 032001]



[arXiv:2211.02491]

X(3872) and X(4014)



- 2003: $X(3872)$, a.k.a. $\chi_{c1}(3872)$, discovered by Belle
[PRL 91 (2003) 262001]
- 2013: quantum numbers determined by LHCb: $J^{PC} = 1^{++}$
[PRL 110 (2013) 222001]
- Its internal structure remains under debate
- Its prompt production in HICs provides an alternative probe to its internal structure

- 2021: $X(4014)$, observed by the Belle collaboration
[PRD 105 (2022) 11, 112011]
- Predicted as the $J^{PC} = 2^{++}$ partner of the $X(3872)$
[Nieves, Pavon Valderrama (2012)]
[Guo, Hidalgo-Duque, Nieves, Pavon Valderrama (2013)]



Investigate these states as heavy meson molecules within the local hidden-gauge symmetry approach
Analyze the in-medium modification

[Cleven, Magas, Ramos (2019)]
[Albaladejo, Nieves, Tolos (2021)]

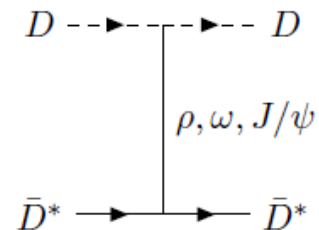
The local hidden-gauge symmetry approach

The interaction is mediated by the exchange of vector mesons

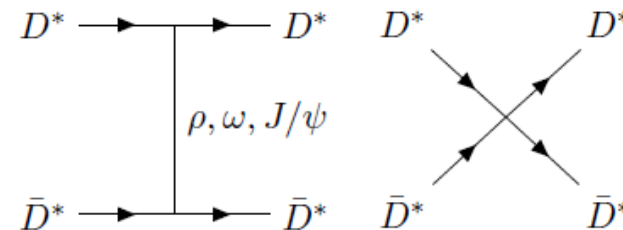
Extended to SU(4), broken by physical masses (exchange of charm is suppressed)

$$\mathcal{L}_{III} = -\frac{1}{4}\langle V_{\mu\nu}V^{\mu\nu}\rangle + \frac{1}{2}m_V^2\left\langle\left(V_\mu - \frac{i}{g}\Gamma_\mu\right)^2\right\rangle$$

$$X(3872) \quad I(J^{PC}) = 0(1^{++}) \quad \left\{ \begin{array}{l} D\bar{D}^* + c.c. \\ D_s\bar{D}_s^* - c.c. \end{array} \right.$$



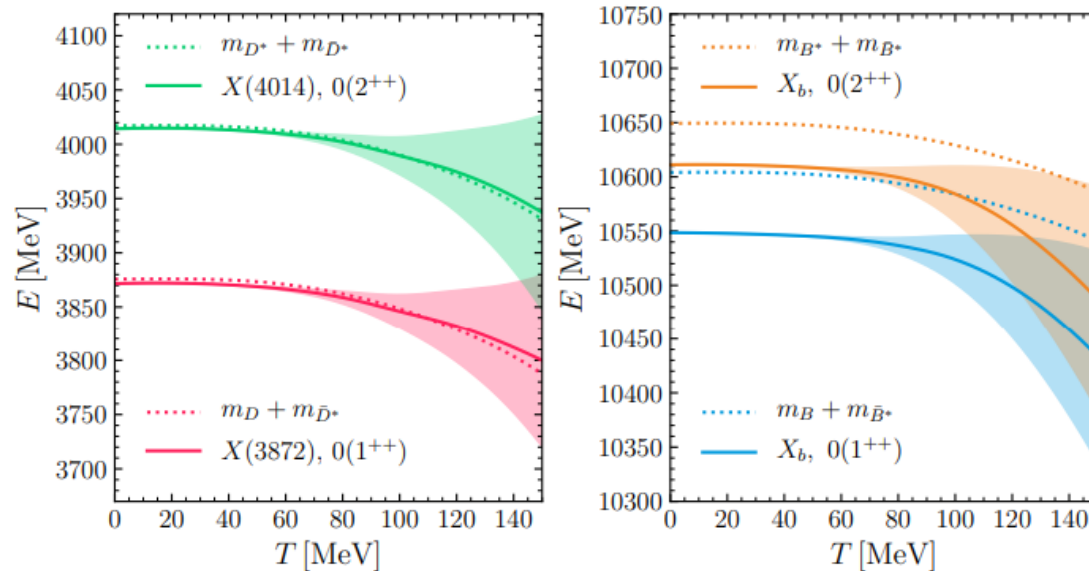
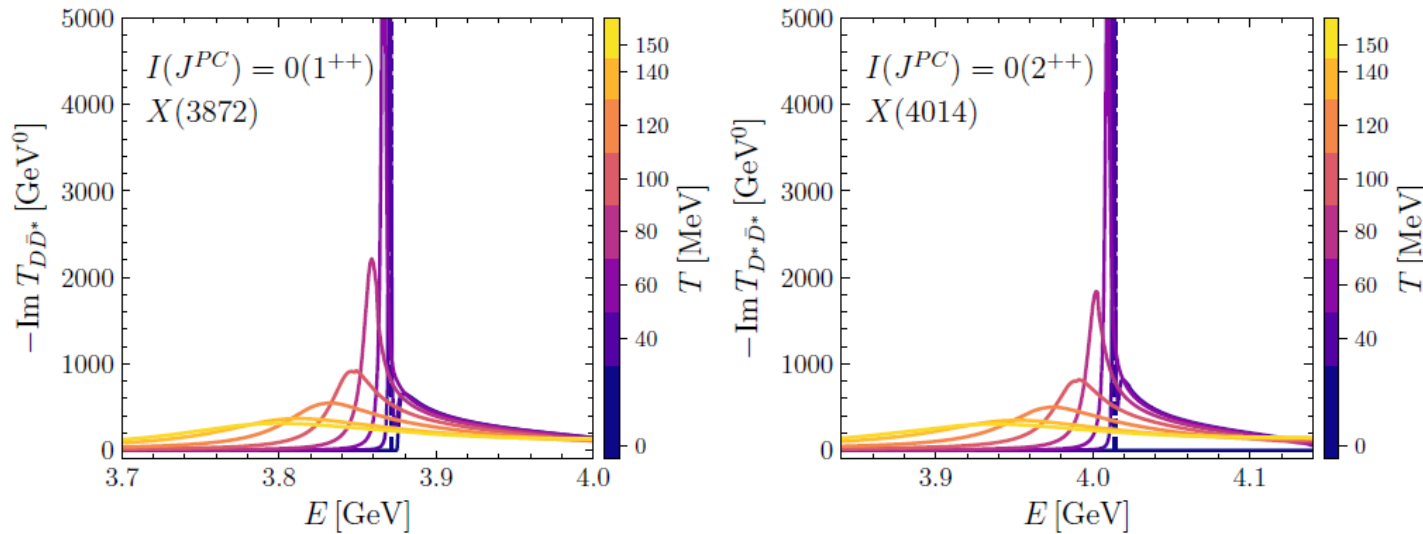
$$X(4014) \quad I(J^{PC}) = 0(2^{++}) \quad \left\{ \begin{array}{l} D^*\bar{D}^* + c.c. \\ D_s^*\bar{D}_s^* - c.c. \end{array} \right.$$



- We obtain the interaction kernel and solve the Bethe-Salpeter equation with G regularized with a cut-off
- The cut-off is fixed in vacuum to reproduce the experimental masses
- At finite temperature, G is dressed with the spectral functions of the D/D_s and D^*/D_s^* mesons

Thermal modification of the X(3872) and X(4014)

[GM, A. Ramos, L. Tolos, J.M. Torres-Rincon,
Phys.Rev.D 107 (2023) 5, 054014]



The masses decrease with increasing temperature

→ drop of the thresholds

Non-zero decay widths at finite

→ widening of open heavy-flavor ground-states

Summary

1. We have extended the EFT describing the scattering of open heavy-flavor mesons off light mesons to finite temperature in a self-consistent way
2. Thermal effects on open heavy-flavor mesons: moderate decrease of the masses and substantial increase of the decay widths with increasing temperature

Similar findings from recent lattice QCD calculations

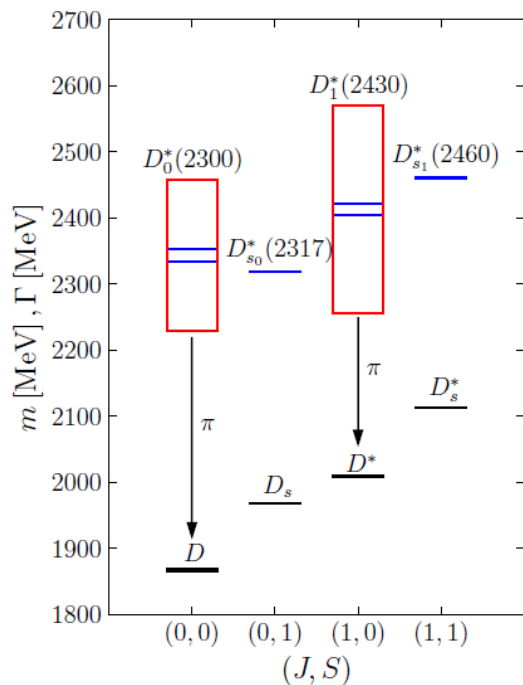
3. We have computed heavy-meson transport coefficients in the hadronic phase from an off-shell kinetic theory including thermal effects

The new contribution coming from the Landau cut of the loop function improves considerably the comparison with lattice QCD calculations and Bayesian analysis.

3. We have studied the finite-temperature modification of the properties of the $X(3872)$ and the $X(4014)$:
 - The masses decrease with temperature (related to the drop of the thresholds $D^{(*)}\bar{D}^*$)
 - Non-zero decay widths at finite temperature (related to the widening of D/\bar{D}^* states)

Backup slides

Results: Dynamically generated states in the charm sector



$D_0^*(2300) : M = 2343 \pm 10 \text{ MeV}$
 $I(J^P) = \frac{1}{2}(0^+) \quad \Gamma = 229 \pm 16 \text{ MeV}$

$D_{s0}^*(2317)^\pm : M = 2317.8 \pm 0.5 \text{ MeV}$
 $I(J^P) = 0(0^+) \quad \Gamma < 3.8 \text{ MeV}$

$D_1(2430)^0 : M = 2412 \pm 9 \text{ MeV}$
 $I(J^P) = \frac{1}{2}(1^+) \quad \Gamma = 314 \pm 29 \text{ MeV}$

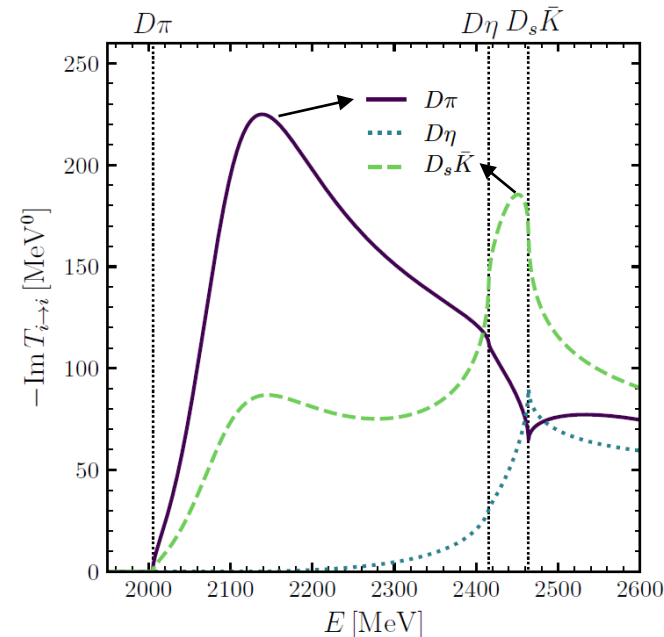
$D_{s1}(2460)^\pm : M = 2459.6 \pm 0.6 \text{ MeV}$
 $I(J^P) = 0(1^+) \quad \Gamma < 3.5 \text{ MeV}$

[PDG (2020)]

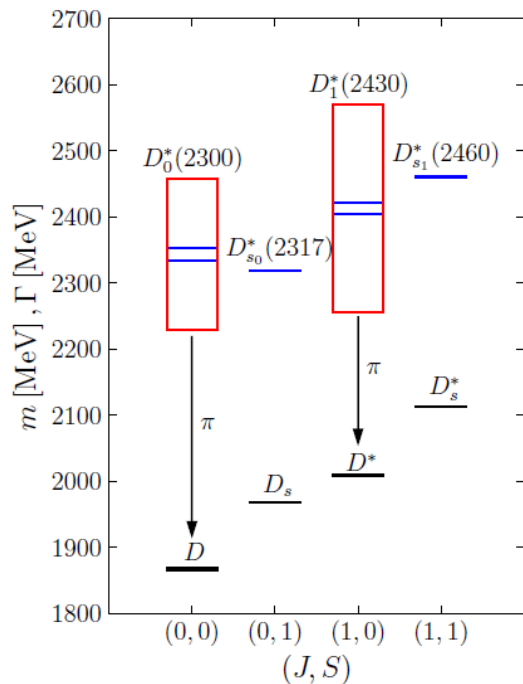
(S, I)	Channels ($J^P = 0^+$)	Threshold (MeV)	Channels ($J^P = 1^+$)	Threshold (MeV)
$(-1, 0)$	$D\bar{K}$	2364.88	$D^*\bar{K}$	2504.20
$(-1, 1)$	$D\bar{K}$	2364.88	$D^*\bar{K}$	2504.20
$(0, \frac{1}{2})$	$D\pi$	2005.28	$D^*\pi$	2146.59
	$D\eta$	2415.10	$D^*\eta$	2556.42
	$D_s\bar{K}$	2463.98	$D_s^*\bar{K}$	2607.84
$(0, \frac{3}{2})$	$D\pi$	2005.28	$D^*\pi$	2146.59
$(1, 0)$	DK	2364.88	D^*K	2504.20
	$D_s\eta$	2516.20	$D_s^*\eta$	2660.06
$(1, 1)$	$D_s\pi$	2106.38	$D_s^*\pi$	2250.24
	DK	2364.88	D^*K	2504.20
$(2, \frac{1}{2})$	D_sK	2463.98	D_s^*K	2607.84

Poles of the unitarized scattering amplitude:

	(S, I)	RS	M_R (MeV)	$\Gamma_R/2$ (MeV)	$ g_i $ (GeV)	χ_i	
Two-pole structure	$D_0^*(2300)$	$(0, \frac{1}{2})$	$(-, +, +)$	2081.9	86.0	$ g_{D\pi} = 8.9$	$\chi_{D\pi} = 0.45$
						$ g_{D\eta} = 0.4$	$\chi_{D\eta} = 0.00$
						$ g_{D_s\bar{K}} = 5.4$	$\chi_{D_s\bar{K}} = 0.02$
		$(-, -, +)$	2529.3	145.4	$ g_{D\pi} = 6.7$	$\chi_{D\pi} = 0.20$	
					$ g_{D\eta} = 9.9$	$\chi_{D\eta} = 0.55$	
					$ g_{D_s\bar{K}} = 19.4$	$\chi_{D_s\bar{K}} = 0.95$	



Results: Dynamically generated states in the charm sector



$$D_0^*(2300) : \quad M = 2343 \pm 10 \text{ MeV}$$

$$I(J^P) = \frac{1}{2}(0^+) \quad \Gamma = 229 \pm 16 \text{ MeV}$$

$$D_{s0}^*(2317)^\pm : \quad M = 2317.8 \pm 0.5 \text{ MeV}$$

$$I(J^P) = 0(0^+) \quad \Gamma < 3.8 \text{ MeV}$$

$$D_1(2430)^0 : \quad M = 2412 \pm 9 \text{ MeV}$$

$$I(J^P) = \frac{1}{2}(1^+) \quad \Gamma = 314 \pm 29 \text{ MeV}$$

$$D_{s1}(2460)^\pm : \quad M = 2459.6 \pm 0.6 \text{ MeV}$$

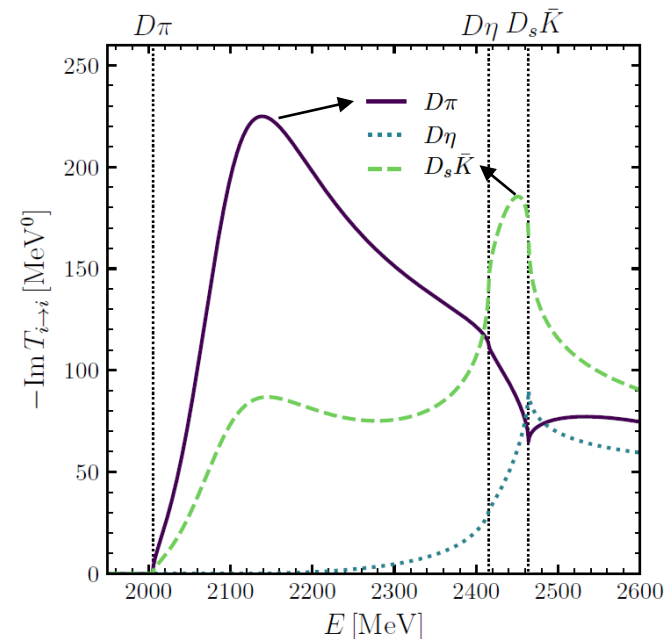
$$I(J^P) = 0(1^+) \quad \Gamma < 3.5 \text{ MeV}$$

[PDG (2020)]

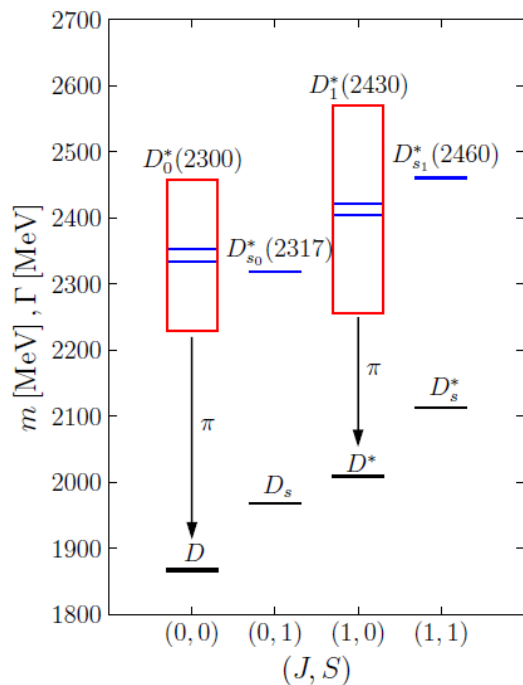
(S, I)	Channels ($J^P = 0^+$)	Threshold (MeV)	Channels ($J^P = 1^+$)	Threshold (MeV)
$(-1, 0)$	$D\bar{K}$	2364.88	$D^*\bar{K}$	2504.20
$(-1, 1)$	$D\bar{K}$	2364.88	$D^*\bar{K}$	2504.20
$(0, \frac{1}{2})$	$D\pi$	2005.28	$D^*\pi$	2146.59
	$D\eta$	2415.10	$D^*\eta$	2556.42
	$D_s\bar{K}$	2463.98	$D_s^*\bar{K}$	2607.84
$(0, \frac{3}{2})$	$D\pi$	2005.28	$D^*\pi$	2146.59
$(1, 0)$	DK	2364.88	D^*K	2504.20
	$D_s\eta$	2516.20	$D_s^*\eta$	2660.06
$(1, 1)$	$D_s\pi$	2106.38	$D_s^*\pi$	2250.24
	DK	2364.88	D^*K	2504.20
$(2, \frac{1}{2})$	D_sK	2463.98	D_s^*K	2607.84

Poles of the unitarized scattering amplitude:

	(S, I)	RS	M_R (MeV)	$\Gamma_R/2$ (MeV)	$ g_i $ (GeV)	χ_i	
Two-pole structure	$D_0^*(2300)$	$(0, \frac{1}{2})$	$(-, +, +)$	2081.9	86.0	$ g_{D\pi} = 8.9$	$\chi_{D\pi} = 0.45$
						$ g_{D\eta} = 0.4$	$\chi_{D\eta} = 0.00$
						$ g_{D_s\bar{K}} = 5.4$	$\chi_{D_s\bar{K}} = 0.02$
						$ g_{D\pi} = 6.7$	$\chi_{D\pi} = 0.20$
						$ g_{D\eta} = 9.9$	$\chi_{D\eta} = 0.55$
Bound state	$D_{s0}^*(2317)$	$(1, 0)$	$(+, +)$	2252.5	0.0	$ g_{DK} = 13.3$	$\chi_{DK} = 0.44$
						$ g_{D_s\eta} = 9.2$	$\chi_{D_s\eta} = 0.08$
						$ g_{D_s\bar{K}} = 19.4$	$\chi_{D_s\bar{K}} = 0.95$



Results: Dynamically generated states in the charm sector



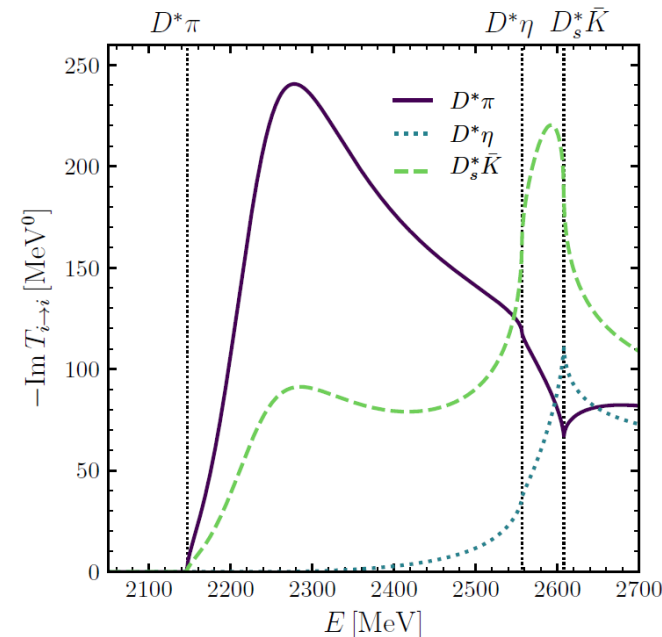
$D_0^*(2300)$:	$M = 2343 \pm 10$ MeV	}
$I(J^P) = \frac{1}{2}(0^+)$	$\Gamma = 229 \pm 16$ MeV	
$D_{s0}^*(2317)^\pm$:	$M = 2317.8 \pm 0.5$ MeV	}
$I(J^P) = 0(0^+)$	$\Gamma < 3.8$ MeV	
$D_1(2430)^0$:	$M = 2412 \pm 9$ MeV	}
$I(J^P) = \frac{1}{2}(1^+)$	$\Gamma = 314 \pm 29$ MeV	
$D_{s1}(2460)^\pm$:	$M = 2459.6 \pm 0.6$ MeV	}
$I(J^P) = 0(1^+)$	$\Gamma < 3.5$ MeV	

[PDG (2020)]

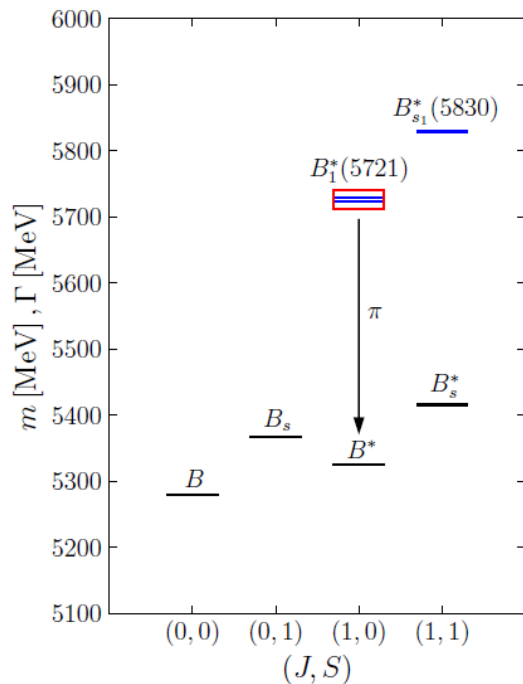
(S, I)	Channels ($J^P = 0^+$)	Threshold (MeV)	Channels ($J^P = 1^+$)	Threshold (MeV)
$(-1, 0)$	$D\bar{K}$	2364.88	$D^*\bar{K}$	2504.20
$(-1, 1)$	$D\bar{K}$	2364.88	$D^*\bar{K}$	2504.20
$(0, \frac{1}{2})$	$D\pi$	2005.28	$D^*\pi$	2146.59
	$D\eta$	2415.10	$D^*\eta$	2556.42
	$D_s\bar{K}$	2463.98	$D_s^*\bar{K}$	2607.84
$(0, \frac{3}{2})$	$D\pi$	2005.28	$D^*\pi$	2146.59
$(1, 0)$	DK	2364.88	D^*K	2504.20
	$D_s\eta$	2516.20	$D_s^*\eta$	2660.06
$(1, 1)$	$D_s\pi$	2106.38	$D_s^*\pi$	2250.24
	DK	2364.88	D^*K	2504.20
$(2, \frac{1}{2})$	D_sK	2463.98	D_s^*K	2607.84

Poles of the unitarized scattering amplitude:

	(S, I)	RS	M_R (MeV)	$\Gamma_R/2$ (MeV)	$ g_i $ (GeV)	χ_i	
Two-pole structure	$D_1(2430)$	$(0, \frac{1}{2})$	$(-, +, +)$	2222.3	84.7	$ g_{D^*\pi} = 9.5$	$\chi_{D^*\pi} = 0.45$
						$ g_{D^*\eta} = 0.4$	$\chi_{D^*\eta} = 0.00$
						$ g_{D_s^*\bar{K}} = 5.7$	$\chi_{D_s^*\bar{K}} = 0.02$
						$ g_{D^*\pi} = 6.5$	$\chi_{D^*\pi} = 0.17$
						$ g_{D^*\eta} = 10.0$	$\chi_{D^*\eta} = 0.54$
Bound state	$D_{s1}(2460)$	$(1, 0)$	$(+, +)$	2393.3	0.0	$ g_{D^*K} = 14.2$	$\chi_{D^*K} = 0.45$
						$ g_{D_s^*\eta} = 9.7$	$\chi_{D_s^*\eta} = 0.08$
						$ g_{D_s^*\bar{K}} = 18.5$	$\chi_{D_s^*\bar{K}} = 0.90$



Results: Dynamically generated states in the bottom sector



$$B_1(5721)^+ : \quad M = 5725.9^{+2.5}_{-2.7} \text{ MeV}$$

$$I(J^P) = \frac{1}{2}(1^+) \quad \Gamma = 31 \pm 6 \text{ MeV}$$

$$B_1(5721)^0 : \quad M = 5726.1 \pm 1.3 \text{ MeV}$$

$$I(J^P) = \frac{1}{2}(1^+) \quad \Gamma = 27.5 \pm 3.4 \text{ MeV}$$

$$B_{s1}(5830)^0 : \quad M = 5828.70 \pm 0.20 \text{ MeV}$$

$$I(J^P) = 0(1^+) \quad \Gamma = 0.5 \pm 0.4 \text{ MeV}$$

[PDG (2020)]

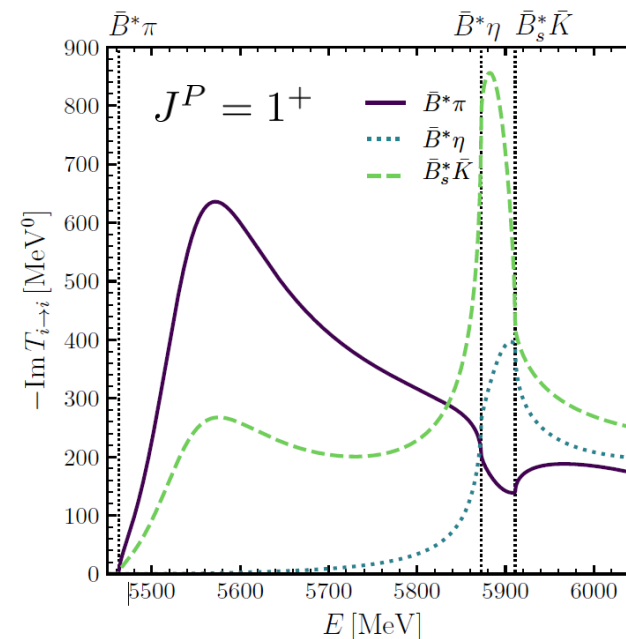
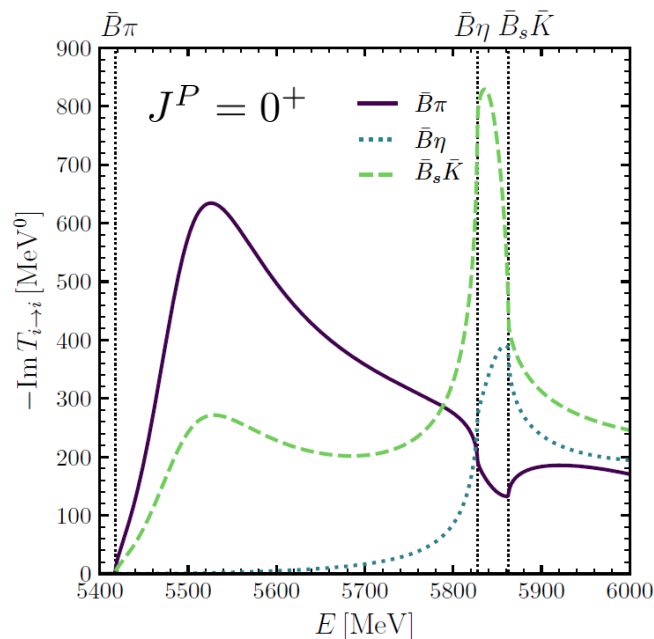
(S, I)	Channels ($J^P = 0^+$)	Threshold (MeV)	Channels ($J^P = 1^+$)	Threshold (MeV)
$(-1, 0)$	$\bar{B}\bar{K}$	5775.12	$\bar{B}^*\bar{K}$	5820.29
$(-1, 1)$	$\bar{B}\bar{K}$	5775.12	$\bar{B}^*\bar{K}$	5820.29
$(0, \frac{1}{2})$	$\bar{B}\pi$	5417.51	$\bar{B}^*\pi$	5462.69
	$\bar{B}\eta$	5827.34	$\bar{B}^*\eta$	5872.51
	$\bar{B}_s\bar{K}$	5862.53	$\bar{B}_s^*\bar{K}$	5911.04
$(0, \frac{3}{2})$	$\bar{B}\pi$	5417.51	$\bar{B}^*\pi$	5462.29
$(1, 0)$	$\bar{B}K$	5775.12	\bar{B}^*K	5820.29
	$\bar{B}_s\eta$	5914.75	$\bar{B}_s^*\eta$	5963.26
$(1, 1)$	$\bar{B}_s\pi$	5504.93	$\bar{B}_s^*\pi$	5553.44
	$\bar{B}K$	5775.12	\bar{B}^*K	5820.29
$(2, \frac{1}{2})$	\bar{B}_sK	5862.53	\bar{B}_s^*K	5911.04

LECs

$$\frac{h_i^B}{\hat{M}_B} = \frac{h_i^D}{\hat{M}_D}, i = \{0, 1, 2, 3\}$$

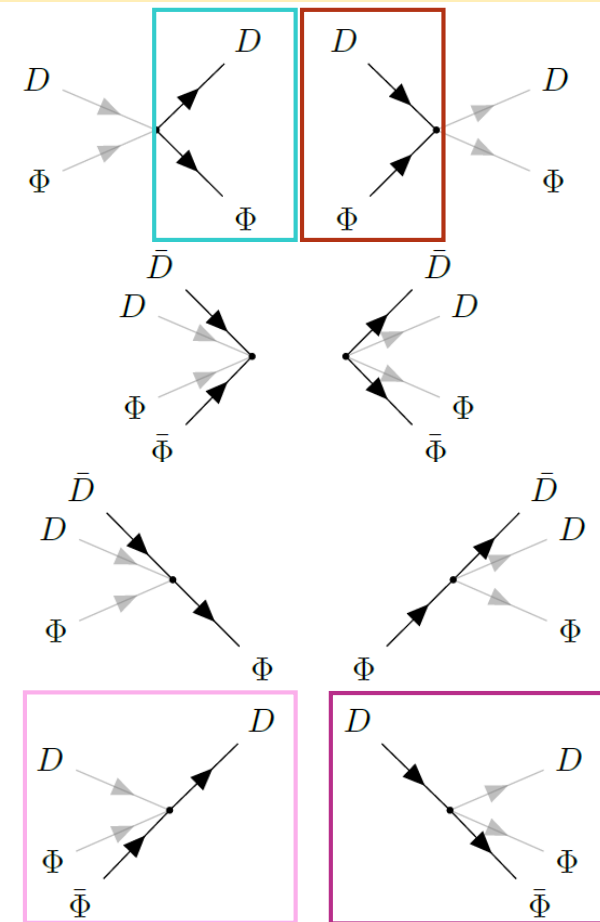
$$h_i^B \hat{M}_B = h_i^D \hat{M}_D, i = \{4, 5\}$$

- Two-pole structure for $(S, I) = (0, \frac{1}{2})$
- Bound state for $(S, I) = (1, 0)$



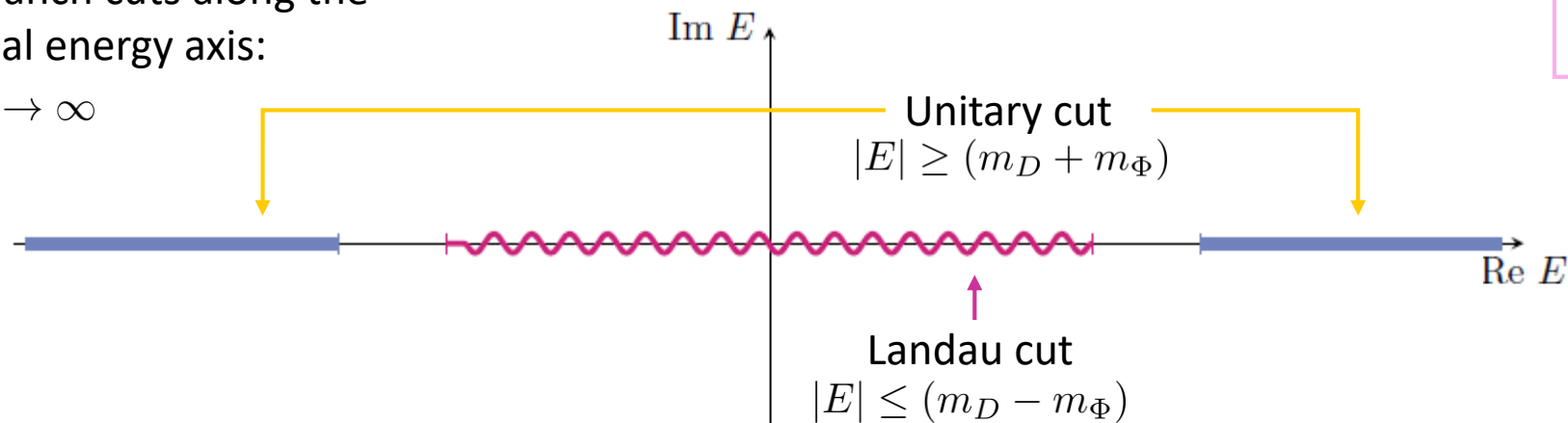
Physical interpretation and cuts of the thermal propagator

$$\begin{aligned}
 \text{Im } G_{D\Phi}(E, \vec{p}; T) = & -\pi \int \frac{d^3q}{(2\pi)^3} \frac{1}{4\omega_D\omega_\Phi} \\
 & \times \left\{ \boxed{[(1+f_D)(1+f_\Phi)]} - \boxed{f_D f_\Phi} \right\} \delta(E - \omega_D - \omega_\Phi) \\
 & + [f_{\bar{D}} f_{\bar{\Phi}} - (1+f_{\bar{D}})(1+f_{\bar{\Phi}})] \delta(E + \omega_D + \omega_\Phi) \\
 & + [f_{\bar{D}}(1+f_\Phi) - (1+f_{\bar{D}})f_\Phi] \delta(E + \omega_D - \omega_\Phi) \\
 & + \left\{ \boxed{(1+f_D)f_{\bar{\Phi}}} - \boxed{f_D(1+f_{\bar{\Phi}})} \right\} \delta(E - \omega_D + \omega_\Phi) \Big\}
 \end{aligned}$$



Branch cuts along the real energy axis:

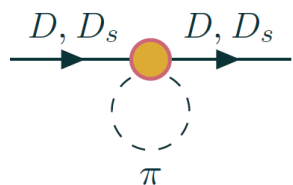
$\Lambda \rightarrow \infty$



Results: Thermal loop functions

[GM, A. Ramos, L. Tolos, J.M. Torres-Rincon, *Phys. Lett. B* 806 (2020) 135464]
 [GM, A. Ramos, L. Tolos, J.M. Torres-Rincon, *Phys. Rev. D* 102 (2020) 9, 096020]

Piononic bath



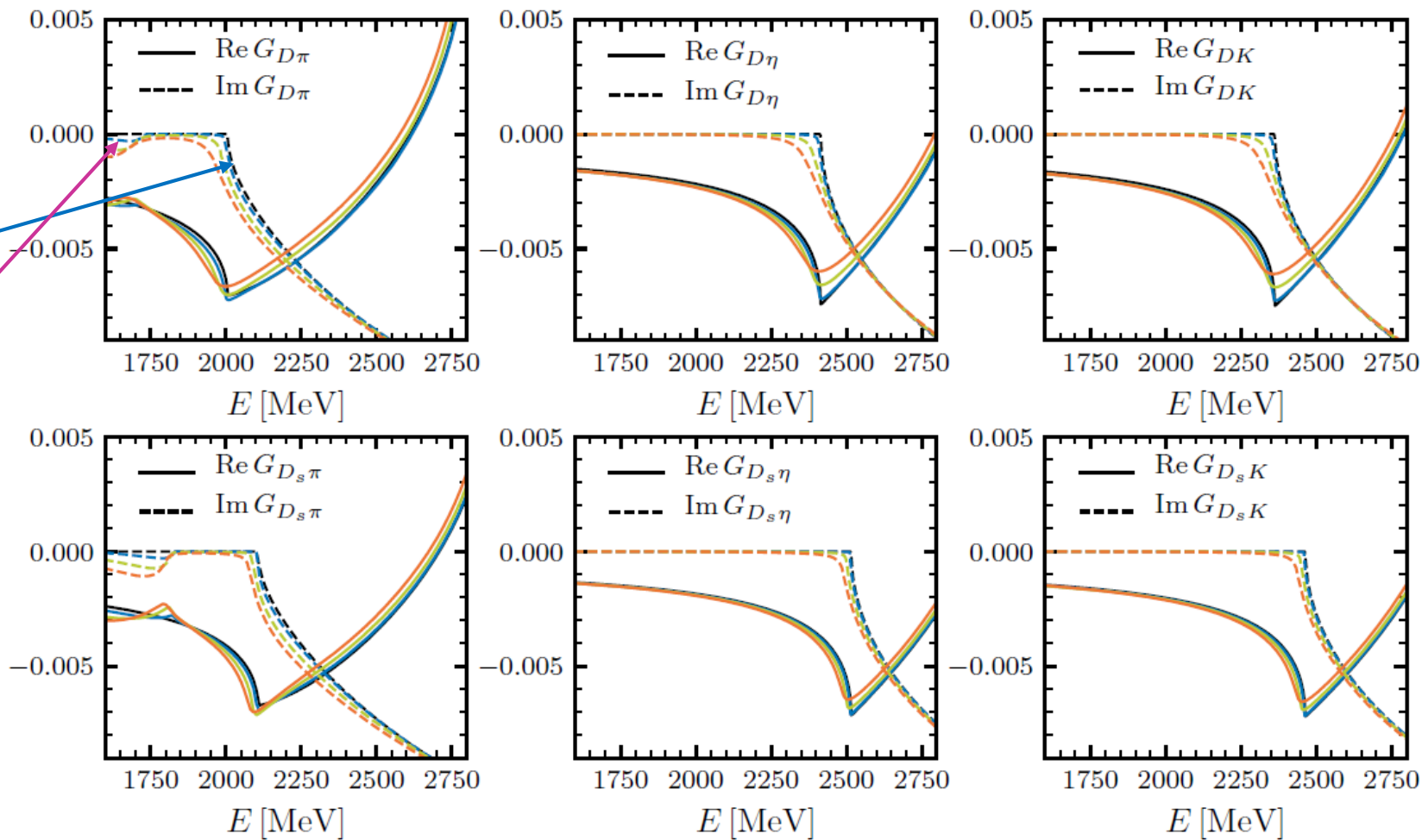
■ $T = 0$ MeV ■ $T = 80$ MeV ■ $T = 120$ MeV ■ $T = 150$ MeV

- Unitary cut

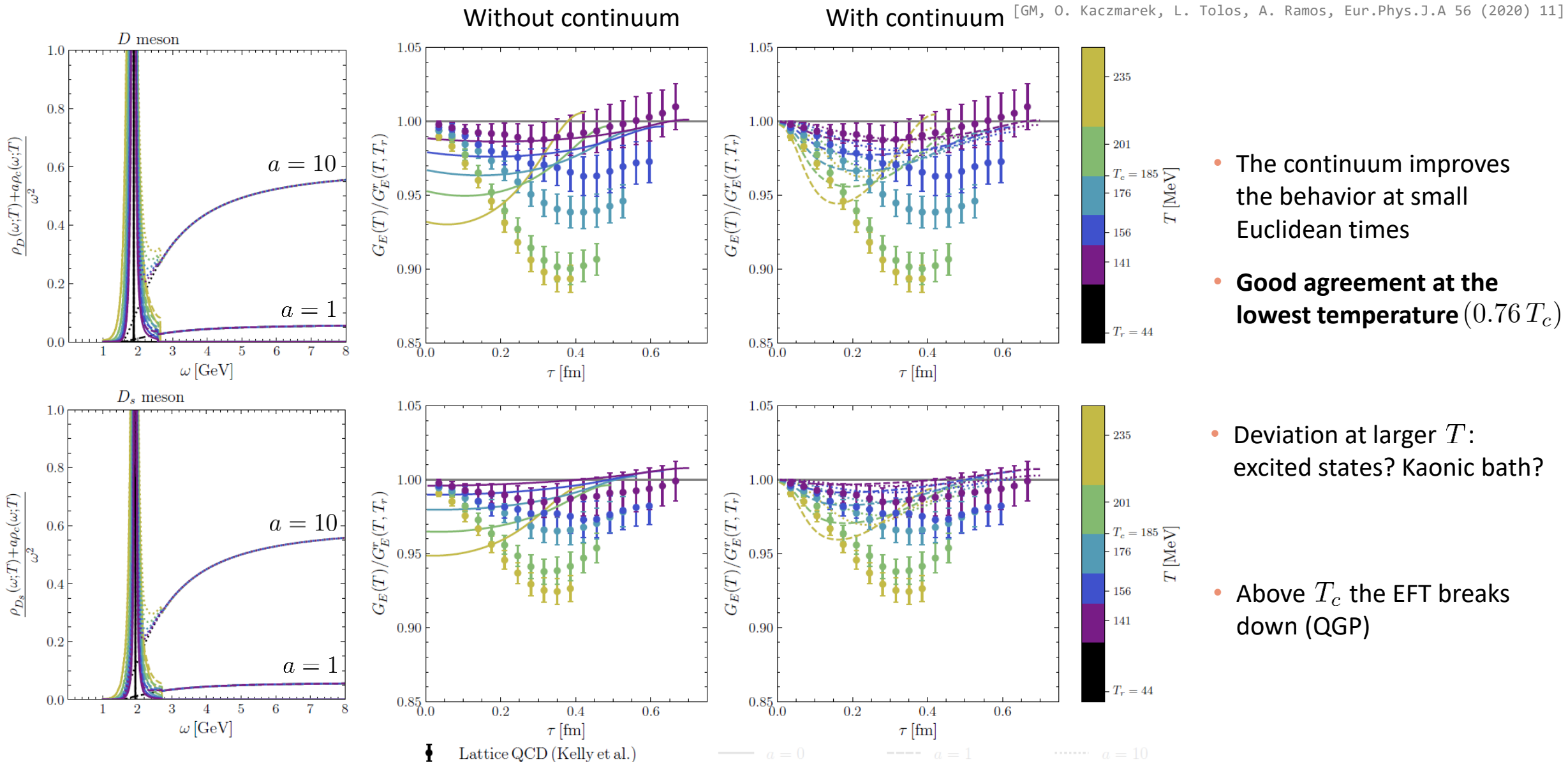
$$|E| \geq (m_D + m_\Phi)$$

- Landau cut

$$|E| \leq (m_D - m_\Phi)$$



Results: Euclidean correlators and comparison with lattice QCD



Results: Comparison with other approaches

[J.M. Torres-Rincon, GM, A. Ramos, L. Tolos, Phys.Rev.C 105 (2022)]

Comparison with:

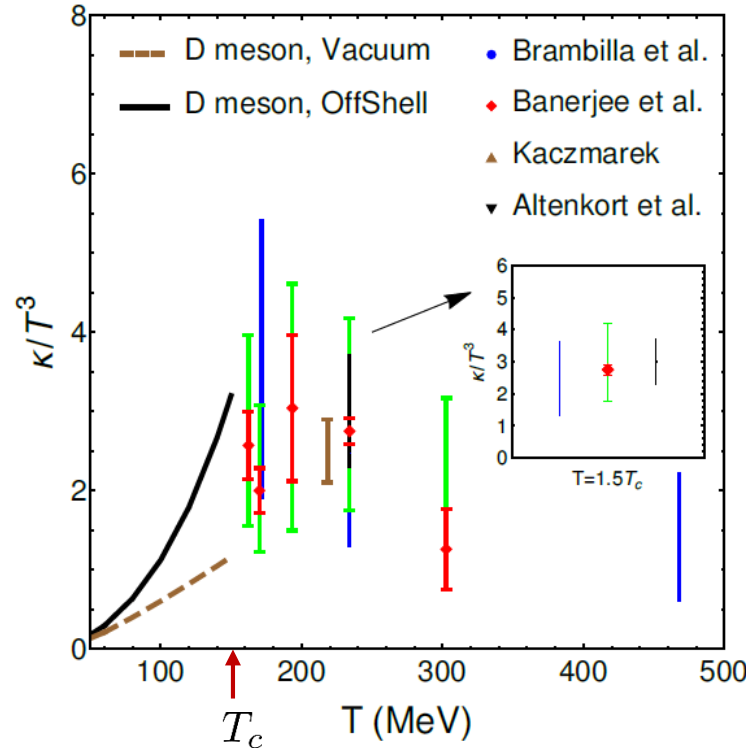
- Lattice QCD calculations

[N. Brambilla et al. Phys. Rev. D102, 074503 (2020)]
 [I.D. Banerjee et al. Phys. Rev. D85, 014510 (2012)]
 [I.A. Francis et al. Phys. Rev. D92, 116003 (2015)]
 [I.L. Altenkort et al. Phys. Rev. D103, 014511 (2021)]

- Bayesian analysis of HICs

[W. Ke et al. Phys. Rev. C98, 064901 (2018)]

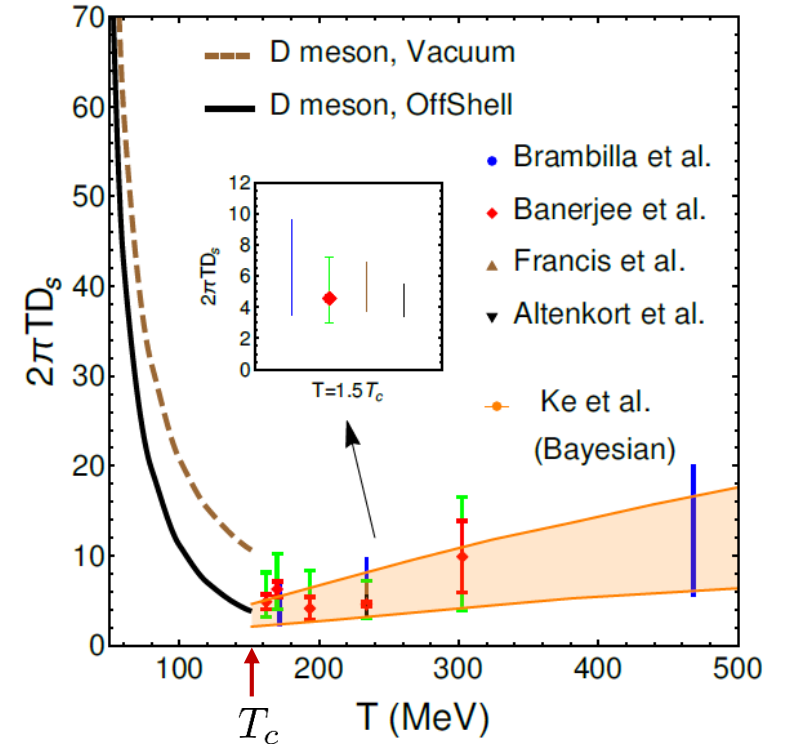
- **Good matching at T_c**
- Important contribution of the **Landau cut** kinetic region



Momentum diffusion coefficient

$$\kappa(T) = \frac{4\pi T^3}{2\pi T D_s(T)}$$

$$\kappa(T) = 2B_0(\vec{k} \rightarrow 0; T)$$



Spatial diffusion coefficient

↳ mean squared displacement of a Brownian particle

$$2\pi T D_s(T) = \lim_{\vec{k} \rightarrow 0} \frac{2\pi T^3}{B_0(\vec{k}; T)}$$